Spatial patterns in glacier area changes from 1962 to 2006 in the Kangchenjunga-Sikkim area, eastern Himalaya

Adina E. Racoviteanu[1,*], Y. Arnaud[1,2], Mark W. Williams[3] and William F. Manley[4]

[1]*Laboratoire de Glaciologie et Géophysique de l'Environnement, 54, rue Molière, Domaine Universitaire, BP 96 38402 Saint Martin d'Hères cedex, France*
[2]*Laboratoire d'Étude des Transferts en Hydrologie et Environnement, BP 53 38401 Saint Martin d'Hères cedex, France*
[3]*Department of Geography and Institute of Arctic and Alpine Research, University of Colorado, Boulder CO 80309*
[4]*Institute of Arctic and Alpine Research, University of Colorado, Boulder CO 80309*

Abstract

This study presents spatial patterns in glacier surface area changes in the Kanchenjunga-Sikkim area of the eastern Himalaya: Nepal (Tamor basin), India (Zemu basin in Sikkim), and parts of China and Bhutan at multiple spatial scales. We combined Corona KH4 and topographic data with more recent remote-sensing data from Landsat 7 Enhanced Thematic Mapper Plus (ETM+), the Advanced Spaceborne Thermal Emission Radiometer (ASTER), QuickBird (QB) and WorldView-2 (WV2) sensors to construct new glacier datasets for this data-scarce area of the Himalaya. We evaluated spatial patterns in glacier surface area changes over almost five decades based on high-resolution datasets (1962 Corona KH4 and 2006 QB data). We investigated the dependency of glacier surface area changes on glacier topography (elevation, slope, aspect, percent debris cover) and climate (solar radiation and precipitation). We also investigated the spatial distribution of supra-glacier temperatures using for several debris-covered glacier tongues based on ASTER data.

Glacier mapping from 2000 Landsat ASTER yielded 1,463 ± 88 km^2 total glacierized area, of which 569 ± 34 km^2 was located in Sikkim. Overall, supraglacial debris covered 11% of the total glacierized area, with regional differences north and south of the topographic divide, and supraglacial lakes covered about 5.8% of the debris-covered glacier area. Based on high-resolution imagery, we estimated an area change of -0.24 ± 0.08% yr^{-1} from 1962 to 2006,

1 with higher rates of area loss for clean glaciers (-34.6%, or -0.7% yr^{-1}) compared to debris-
2 covered glaciers (-14.3% or -0.3 yr^{-1}). Some debris covered glacier tongues experienced less
3 area changes, and appear to have stable termini. Glaciers in the Kangchenjunga-Sikkim area
4 are losing area at rates similar to those reported for the last decades in the Himalaya, but
5 individual glacier rates of change are heterogenous, and vary within the study area with
6 respect to local topography, percent debris cover or glacier elevations.
7

8 ## 1. Introduction

9
10 Himalayan glaciers have generated a lot of concern in the last few years, particularly with
11 respect to glacier area and elevation changes and their consequences for the regional water
12 cycle (Immerzeel et al. 2010; Kaser et al. 2010; Immerzeel et al. 2012; Racoviteanu et al.
13 2013a). Remote sensing techniques have helped improve estimates of glacier area changes
14 (Bajracharya et al. 2007; Bolch 2007; Bolch et al. 2008a; Bhambri et al. 2010; Kamp et al.
15 2011), glacier lake changes (Wessels et al. 2002; Bajracharya et al. 2007; Bolch et al. 2008b;
16 Gardelle et al. 2011) and region-wide glacier mass balance (Berthier et al. 2007; Bolch et al.
17 2011; Kääb et al. 2012; Gardelle et al. 2013), but significant gaps do remain. The new global
18 Randolph inventory v.4 (Pfeffer et al. 2014) provides a global dataset of glacier outlines
19 intended for large-scale studies; however, in some regions the quality varies, and the outlines
20 may not be suitable for detailed regional analysis of glacier parameters. Regional glacier
21 inventories have been constructed recently, for example for the western part of the Himalaya
22 (e.g. Bhambri et al. 2011; Kamp et al. 2011; Frey et al. 2012), but only a few are available for
23 the eastern extremity of the Himalaya (e.g. Bahuguna 2001; Krishna 2005; Bajracharya and
24 Shrestha 2011; Basnett et al. 2013). The use of remote sensing for glacier mapping in this
25 area is limited by frequent cloud cover and sensor saturation due to unsuitable gain settings

and the persistence of seasonal snow, which hampers quality satellite image acquisition. Furthermore, this area has very limited baseline topographic data needed for comparison with recent satellite-based data, as discussed in detail in Bhambri and Bolch (2009a). The earliest Indian glacier maps date from topographic surveys conducted by expeditions in the mid-nineteenth century (Mason 1954), but these are limited to a few glaciers. The Geologic Survey of India (GSI) inventory based on 1970s Survey of India maps (Shanker 2001; Sangewar and Shukla 2009) is not in the public domain. For eastern Nepal, 1970's topographic maps from Survey of India 1:63,000 scale are available, but their accuracy is not known with certainty. Given these limitations, declassified Corona imagery from the 1960s and 1970's has increasingly been used to develop baseline glacier datasets, such as in the Tien Shan (Narama et al. 2007), Nepal Himalaya (Bolch et al. 2008a) and parts of Sikkim Himalaya (Raj et al. 2013).

The topographic and climatic controls on glacier surface area and elevation changes across the Himalaya has received increasing attention in recent studies, particularly with respect to the role of debris cover (Bolch et al. 2008a; Salerno et al. 2008; Basnett et al. 2013; Thakuri et al. 2014). Some studies have characterized the small-scale glacier surface topography using field-based surveys (Iwata et al. 2000; Sakai and Fujita 2010; Zhang et al. 2011). Some understanding of these patterns at mountain-range scale, however, is starting to emerge (Scherler et al. 2011; Bolch et al. 2012; Gardelle et al. 2013; Racoviteanu et al. 2014). Overall glacier shrinkage and mass loss has been documented throughout the Himalaya, concomitantly with an increase in debris cover (Bolch et al. 2011; Nuimura et al. 2012). However, the influence of debris cover on glacier mass balance remains debatable (Scherler et al. 2011; Kääb et al. 2012), and modeling of melt under the debris cover is subject to uncertainties (Mihalcea et al. 2008a; Mihalcea et al. 2008b; Zhang et al. 2011; Foster et al. 2012). Updated, accurate glacier inventories are continuously needed to understand the

climatic, topographic and glacier parameters that govern glacier fluctuations across the Himalaya.

In this study, we constructed updated glacier inventories for this poorly investigated area of the eastern Himalaya from multi-temporal satellite data: Corona KH4, Landsat 7 Enhanced Thematic Mapper Plus (ETM+), the Advanced Spaceborne Thermal Emission Radiometer (ASTER), QuickBird (QB) and WorldView-2 (WV2) sensors along with elevation data from the Shuttle Radar Topography Mission (SRTM). While the main goal is to provide estimates of the current glacier distribution and parameters in this area, we also aim at understanding spatial patterns in glacier surface area changes in the last decades and their dependence on topographic and climatic factors. Particular emphasis is placed on surface characteristics of debris-covered glacier tongues, using ASTER-derived surface temperature as a proxy. These updated glacier datasets help fill a gap in regional glacier inventories and may provide a baseline for future mass balance investigations where accurate glacier outlines are needed.

2. Study area

The study area encompasses glaciers in the eastern Himalaya (27° 04' 52" N to 28° 08' 26" N latitude and 88° 00' 57" E to 88° 55' 50" E longitude), located on either side of the border between Nepal and India in the Kangchenjunga-Sikkim area (Fig. 1). Based on SRTM data, relief in this area ranges from 300 m at the bottom of the valleys to 8,598 m (Mt. Kanchenjunga), Valley glaciers cover about 68% of the glacierized area, mountain glaciers cover 28%, and the remaining are cirque glaciers and aprons (Mool et al. 2002). The glacier ablation area is typically covered by heavy debris-cover originating from rockfall on the steep slopes (Mool et al. 2002), reaching up to a thickness of several meters at the glacier termini (Kayastha et al. 2000). The eastern part of this area constitutes the Sikkim province of India, and the western part is located in eastern Nepal, and encompasses the Tamor and parts of Arun basin. Climatically, this area of the Himalaya is dominated by the South Asian summer

monsoon circulation system (Bhatt and Nakamura 2005) caused by the inflow of moist air from the Bay of Bengal to the Indian subcontinent during the summer (Yanai et al. 1992; Benn and Owen 1998). The Himalaya and Tibetan plateau (HTP) acts as a barrier to the monsoon winds, bringing about 77% of precipitation on the south slopes of the Himalaya during the summer months (May to September) (Fig. 2). This climatic particularity causes a "summer-accumulation" glacier regime type, with accumulation and ablation occurring simultaneously in the summer (Ageta and Higuchi 1984). In Sikkim, rainfall amounts range from 500 to 5000 mm per year, with annual averages of 3,580 mm recorded at Gangtok station (1,812 m) (1951 to 1980) (IMD 1980), and 164 rainy days per year (Nandy et al. 2006). Mean minimum and maximum daily temperatures at Gangtok station were reported as 11.3°C and 19.8°C, with an average of 15.5°C based on the same observation record (IMD 1980).

[Fig. 1 – 2]

3. Methodology

3.1. Data sources

Satellite imagery

Remote sensing datasets used in this study are summarized in Table 1, and included: 1) baseline remote sensing data for the 1960s decade from Corona declassified imagery (year 1962); 2) "reference" datasets for 2000s from Landsat ETM+ and ASTER and 3) high-resolution imagery from QB (2006) and WV (2009), all described below.

(1) Corona KH4 scenes (1962*)* were obtained from the US Geological Survey EROS Data Center (USGS-EROS 1996). The Corona KH4 system was equipped with two panoramic cameras (forward-looking and rear-looking with 30 degrees separation angle), and acquired imagery from February 1962 to December 1963 (Dashora et al. 2007). We chose images

from the end of the ablation season (October/November in this part of the Himalaya), suitable for glaciologic purposes. Six Corona stripes were scanned at 7 microns by USGS from the original film strips, with a reported nominal ground resolution of 7.62 m (Dashora et al. 2007). Corona images are known to contain significant geometric distortions due cross-path panoramic scanning. The Frame Ephemeris Camera and Orbital Data (FECOD) camera/spacecraft parameters (roll, pitch, yaw, speed, altitude, azimuth, sun angle and film scanning rate) for Corona missions, needed to construct a camera model and to correct these distortions, are not easily available. To orthorectify the scenes, we defined a non-metric camera model in ERDAS Leica Photogrammetric Suite (LPS), with focal length, air photo scale and flight altitude extracted from the declassified documentation of the KH4 mission (Dashora et al. 2007). We used the bundle block adjustment procedure in LPS to simultaneously estimate the orientation of all the CORONA stripes on the basis of 117 ground control points (GCPs) extracted from the panchromatic band of the 2000 Landsat ETM+ image (15 m spatial resolution). GCPs were identified on the Landsat image on non-glacierized terrain including moraines, river crossings, and outwash areas. Tie points (TPs) were manually digitized on overlapping Corona strips and on the Landsat image. Elevations were extracted from the SRTM DEM v.4 (CGIAR-CSI 2004) and were used to correct effects of topographic terrain displacements. The Corona stripes were mosaicked in ERDAS LPS to produce the final orthorectified image, with a horizontal accuracy (RMSEx,y) of the bundle block adjustment of 10.5 m.

(2) The orthorectified Landsat ETM+ scene from December 2000, obtained from the USGS Eros Data Center was the main dataset for the updated glacier inventory. The Landsat ETM+ scene has seven spectral channels at 30 m spatial resolution, a thermal channel at 60 m and a panchromatic channel at 15 m, a revisit time of 16 days and a large swath width (185 km). In addition, six orthorectified ASTER products (2000 to 2002) were obtained at no cost

through the Global Land Ice Monitoring from Space (GLIMS) project (Raup et al. 2007). The ASTER scenes have 3 channels in the visible wavelengths (15 m spatial resolution), 3 channels in the short-wave infrared at 30 m, and four thermal channels at 90 m, a swath width of 60 km and a revisit time of 16 days. Images were selected at the end of the ablation season for minimal snow, and had little or no clouds. Five of these scenes were used for on-screen manual corrections of the Landsat-based glacier outlines in challenging areas where shadows or clouds obstructed the view of the glaciers. In addition, the surface kinetic temperature product (AST08) product from the November 27th, 2001 ASTER scene was used for clean ice delineation of debris cover along with topographic information using a decision-tree algorithm (Racoviteanu and Williams 2012). The October 29th, 2002 scene, covering the Kanchenjunga-Sikkim area east and west of the topographic divide, was used to investigate the spatial distribution of surface temperature over selected debris covered tongues.

(3) Two QB scenes from January 2006 were obtained from Digital Globe as ortho-ready standard imagery (radiometrically calibrated and corrected for sensor and platform distortions) (Digital_Globe 2007). These scenes, covering an area of 1,107 km^2 were well-contrasted and mostly snow-free outside the glaciers. We orthorectified these scenes in ERDAS Imagine Leica Photogrammetry Suite (LPS) using Rational Polynomial Coefficients (RPCs) provided by Digital Globe and the SRTM DEM, and mosaicked them in ERDAS Imagine. The scenes were resampled to 3 m-pixel size during the orthorectification process using the cubic convolution method suitable for continuous raster data, in order to reduce disk space and processing time. One WorldView-2 (WV2) panchromatic, ortho-ready scene at 50 cm spatial resolution from Dec 02, 2010 was also obtained to cover the terminus of Zemu glacier, which was missing from the QB extent. All datasets were registered to UTM projection zone 45N, with elevations referenced to the WGS84 datum.

[Table 1]

Elevation datasets

Two elevation datasets were used in this study:

(1) The hydrologically-sound, void-filled CGIAR SRTM DEM (90 m spatial resolution) (CGIAR-CSI 2004) was used to extract glacier parameters for 2000. The SRTM dataset is known to have biases on steep slopes and at higher elevations (Berthier et al. 2006; Fujita et al. 2008; Nuth and Kääb 2011), as well as due to radar penetration on snow (Gardelle et al. 2012). For this area, the vertical accuracy of the SRTM DEM, calculated as root mean square (RMSEz) with respect to 25 field-based GCPs, was 31 m ± 10 m. The GCPs were obtained in the field on non-glacierized terrain including roads and bare land outside the glaciers using a Trimble Geoexplorer XE series.

(2) The Swiss topographic map (1:150,000 scale), compiled from Survey of India maps from the 1960s, published by the Swiss Foundation for Alpine Research was used for manual corrections of the 1962 Corona glacier outlines. The exact month or year of each quadrant, or of the original air photos is not known with certainty because the original large-scale Indian topographic maps at this scale are restricted within 100 km of the Indian border, and are therefore inaccessible (Srikantia 2000; Survey_of_India 2005).

3.2 Analysis extents

We defined two spatial domains for our study area (Fig. 1). *Spatial domain 1* includes the Sikkim province of India, eastern Nepal (Tamor and Arun basins), as well as parts of Bhutan and China (Table 2).

[Table 2]

This spatial domain was split into four sub-regions on the basis of east-west and north-south climate/topographic/political barriers, as shown in Fig. 3. Rainfall averages from the Tropical Rainfall Measuring Mission (TRMM) data 2B31 product (Bhatt and Nakamura

2005; Bookhagen and Burbank 2006) were used to characterize the sub-regions climatically. The dataset contains rainfall estimates calibrated with ground-control stations derived from local and global gauge stations (Bookhagen and Burbank 2006) with a spatial resolution of 0.4 degree, or ~5 km. Given the well-known biases in the TRMM data (Bookhagen and Burbank 2006; Andermann et al. 2011; Palazzi et al. 2013), here we are not concerned with the absolute values of gridded precipitation, but only with characterizing the sub-regions in our study area using relative rainfall values. TRMM data integrated over 10 years (1998 to 2007) show differences in precipitation patterns among the four regions, and justifies our choice of spatial domains (Table 3). The eastern side of the study area (Sikkim) receives higher precipitation amounts than the western side (Nepal) (977 mm/yr versus 805 mm/yr). There is a pronounced north-south gradient in precipitation, with the lowest amount of precipitation noticeable on the China side (146 mm/yr) (Table 3).

[Fig. 3 and Table 3]

Spatial domain 2 is a subset of spatial domain 1, and represents 50 glaciers from the Tamor basin (Nepal) and Zemu basin (Sikkim, India), located on the southern slopes of the Himalaya and comprising of clean as well as debris-covered glaciers. Recent studies (Thakuri et al. 2014) pointed out the variability in glacier terminus and elevation changes between the northern and southern slopes of the Himalaya. To facilitate comparison with this study and others from the same climatic area, we excluded glaciers from China and Bhutan from the glacier area change analysis. Glacier surface area changes were computed between two time steps: the 1960s decade (represented by Corona imagery), and 2000s decade (represented by QB and WV2). The dependence of glacier area changes on climatic and topographic variables extracted from 2000 elevation data was investigated using correlation analysis.

3.3 Glacier delineation and analysis

For the 1960s, clean glacier outlines were extracted from the panchromatic Corona imagery by thresholding the digital numbers (DN > 200 = snow/ice), chosen based on visual interpretation. Debris-covered glacier tongues were delineated manually on the basis of lateral moraines and other visual clues such as supra-glacial lakes. A 5x5 median filter was used to remove noise (isolated pixels from snowfields or internal rocks), as recommended in other studies (Andreassen et al. 2008; Racoviteanu et al. 2009). Ice polygons with area <0.02 km^2 were not considered valid glaciers and were excluded from the analysis. Manual corrections were applied subsequently on the basis of the topographic map using on-screen digitizing in areas of poor contrast or transient snow/clouds, which obstructed the view of glaciers.

For the 2000s, glaciers were delineated from the Landsat ETM+ scene using the Normalized Difference Snow Index (NDSI) (Hall et al. 1995), with a threshold of 0.7 (NDSI > 0.7 = snow/ice). The NDSI algorithm relies on the high reflectivity of snow and ice in the visible to near infrared (VNIR) wavelengths (0.4 – 1.2 μm), compared to their low reflectivity in the shortwave infrared (SWIR, 1.4 - 2.5 μm) (Dozier 1989; Rees 2003). Compared to other band ratios (Landsat ¾ and $^3/_5$), the NDSI glacier map was cleaner and less noisy and was therefore preferred (Racoviteanu et al. 2008b). A 5x5 median filter was used here as well to remove remaining noise, and a few areas were adjusted manually on the basis of the ASTER images, notably frozen lakes misclassified as snow/ice, and some glaciers underneath low clouds in the southern part of the image. Some transient snow persisting in the deep shadowed valleys was manually removed from the glacier outlines on the basis of the topographic map. Debris-covered glacier tongues were delineated using multispectral data (band ratios, surface kinetic temperature and texture) from the Nov 27,

2001 ASTER scene combined with topographic variables in a decision tree, as described in Racoviteanu and Williams (2012).

For the QB (2006) image, clean ice surfaces were delineated using band ratios ¾, then isodata clustering with a threshold of 1.07 (snow/ice > 1.07), and a majority filter of 7x7 to remove noise. Debris-covered tongues for this dataset were delineated manually on the basis of supraglacial features (lakes and ice walls), along with lateral and frontal moraines visible on the high resolution images. We also mapped supraglacial lakes from this high-resolution data based on band ratios, along with texture analysis.

For all inventories in spatial domain 1, ice masses were separated into glaciers on the basis of the SRTM DEM, using hydrologic functions in an algorithm developed by Manley (2008), described in Racoviteanu et al. (2009). Glacier area, terminus elevation, maximum and median elevation, average slope angle and aspect were extracted on a glacier-by-glacier basis using zonal functions. Average glacier thickness were calculated from mass turnover principles and ice flow mechanics Huss and Farinotti (2011), based on the approach of Farinotti (2009). Their method uses glacier outlines and the SRTM DEM to derive thickness estimates iteratively based on Glenn's flow law and a shape factor (Paterson 1994). For simplicity and consistency for change analysis, we assumed no shift in the ice divides over the period of analysis, and excluded all nunataks and snow-free steep rock walls from the glacier area calculations. Bodies of ice above the bergschrund were considered part of the glacier (Raup and Khalsa 2007; Racoviteanu et al. 2009). Glacier area changes (1962 to 2000) and their dependency on topographic and climatic variables were calculated on a glacier-by-glacier basis for the 50 glaciers in spatial domain 2.

3.4 Uncertainty estimates

Glacier outlines derived from remote sensing data at various spatial and temporal resolution are known to be subject to various degrees of uncertainty, as discussed in recent

studies (Racoviteanu et al. 2009; Paul et al. 2013). This becomes an important issue in glacier change analysis, where errors from various data sources accumulate at each processing step. The main sources of uncertainty here are: 1) errors inherent in the source data (geolocation errors, sensor limitations and ambiguity in the satellite signal), 2) image classification errors (positional errors and/or errors due to the semi-automated glacier mapping method); 3) conceptual errors associated with the definition of a glacier, including mapping of ice divides, mixed pixels of snow and clouds, and internal rock differences, all described in detail in Racoviteanu et al. (2009). Here we ignored errors due to atmospheric and topographic effects, resampling techniques, image co-registration, spectral mixing or raster to vector conversion. The error in glacier surface area change (E) was computed from the errors due to rock inconsistencies (E_{rock}) and classification errors ($E_{classif}$) embedded in each dataset as the RMSE, explained below:

$$E = \sqrt{E^2_{rock} + E^2_{classif}}$$

(1) *Geolocation errors:* The orthorectification process of the 1962 Corona yielded a RMSEx,y error of ± 10 m. We performed an independent analysis of location accuracy using 30 check points chosen independently of the initial GCPs, which yielded an actual "ground" RMSEx,y of the Corona block of ~60 m. This is consistent with accuracies obtained on Corona images in Mexico, using a fitting software and the FECOD parameters (Henry Snyder, NASA Goddard, personal communication, 2011). A trend analysis on the horizontal shifts between Corona and the reference Landsat scene showed that the largest errors were concentrated towards the edges of the images, mostly outside the glaciers, and did not impact the differences in glacier area, therefore were not included in the error estimates for change analysis. For the QB scenes, the geolocation accuracy is reported as $RMSE_{x,y}$ of 14 m globally (Digital_Globe 2007).

(2) *Image classification errors:* The accuracy of remote sensing glacier outlines was estimated using the "Perkal epsilon band" around glacier outlines (Racoviteanu et al. 2009; Bolch et al. 2010), using a ~1-pixel variability (Congalton 1991). Using the 1-pixel variability (±30 m for Landsat/ASTER, ±6 m for Corona and ±3 m for QB outlines), we obtained a total estimate of image classification errors of 3 – 6% for our datasets, with the highest uncertainties associated with the larger pixel size (Landsat). The method is known to slightly over-estimate the errors described in Burrough and McDonnel (1998), so we consider our overall area accuracy estimates to be rather conservative, and to accommodate other errors not considered here (higher uncertainty of debris-covered tongues, GIS operations etc.). Recent glacier analysis comparison experiments reported a range of uncertainty of < 5% for remote sensing glacier outlines compared to high-resolution imagery (Raup et al. 2007; Paul et al. 2013). For manually-adjusted glacier outlines, particularly debris-covered tongues, we used screen digitizing in streaming mode, with a high density of vertices, recently shown to minimize area errors (B. Raup, National Snow and Ice Data Center, personal communication, 2014).

(3) *Conceptual errors:* To ensure consistency among the various datasets, we removed internal rocks from all the area calculations; we manually removed perennial snowfields from the glaciers and we included "inactive" bodies of ice above the bergschrund as part of a glacier (Racoviteanu et al. 2009). Uncertainties due to different digitization of internal rocks were derived by comparing area changes computed with internal rocks specific to each dataset, versus "merged" internal rocks from each datasets. The differences in glacier datasets due to rock inconsistencies amounted to ~2 % glacier area, inducing differences in the rates of change in area of ± 0.05% yr^{-1}. For the change analysis, to minimize uncertainties due to differences in rock outcrops specific to each dataset, we merged rock outcrops from each

dataset and applied to each time step. For simplicity, we neglected the area change that might be due to exposure of new internal rock due to glacier ice thinning.

The total uncertainties for the three datasets, calculated as $RMSE_{x,y}$ amounted to ± 3%, ±6 and ±3 % of the glacierized area for Corona, Landsat/ASTER and QuickBird respectively.

4. Results

4.1 The Landsat/ASTER 2000 glacier patterns (Spatial domain 1)

The 2000 glacier inventory based on Landsat and ASTER yielded 487 glaciers (of which 162 were situated in Nepal, 186 in Sikkim, 30 in Bhutan and 109 in China), covering a total surface area of 1463 ± 88 km^2 (Table 4a). Of the 487 glaciers in this spatial domain, 68 glaciers (13%) had debris cover on the ablation area of their tongues. Supraglacial debris covered 160 ± 10 km^2 (11% of the glacierized area in spatial domain 1), with some differences between north and south slopes of the study area. In Sikkim, supraglacial debris covered an area of 78 ± 5 km^2 in 2000 (14% of the glacierized area). The percent debris cover estimated here is lower than those reported for other areas of the southern slopes of the central Himalaya by Scherler et al. (2011) (36% debris cover), or from the Khumbu region, west of our study area, by Fujii and Higuchi (1977), Nuimura et al. (2012) (34.8%), Racoviteanu et al. (2013a) (27 %) and Thakuri et al. (2014) (32%).

Debris cover is more prevalent on the southern side of the divide (Sikkim, 14% of glacierized area) compared to the northern one (China, 2% of the glacierized area), perhaps due to different geologic and topographic patterns. The northern side of the divide, which is part of the Tibetan plateau, is situated in a monsoon shadow and is therefore dry; the gentler slopes induce lower rates of erosion. In contrast, the southern slopes of the Himalaya receive large amounts of monsoon moisture; the steep slopes are made of soft sedimentary rocks and Precambrian crystalline rocks (Mool et al. 2002) and are prone to high rates of erosion. This

north-south difference in debris cover amounts was also noted in other studies (Scherler et al. 2011).

[Table 4 a-b]

In 2000, glacier size ranged from 0.02 – 105 km^2, with an average size of 3 km^2 and a median size of 0.9 km^2 (Table 4b). In the Khumbu region, west of our study area, glaciers tend to be smaller on average (1.4 km^2) (Bajracharya and Shrestha 2011). The histogram of glacier area (Fig. 4a) is skewed to the right (skewness = 8.4), showing that glaciers with area < 10 km^2 are predominant in this region, and glacier size decreases non-linearly. The long right-tail extremes represent only a few glaciers such as Zemu, with an area > 100 km^2. The prevalence of small glaciers is a fairly common pattern worldwide, also observed for the Cordillera Blanca of Peru in a previous study (Racoviteanu et al, 2008a).

[Fig. 4 a-d]

Glacier termini elevations in spatial domain 1 ranged from 3,990 to 5,777 m, with a mean of 4,908 m; median glacier elevation ranged from 4,515 to 6,388 m, with a mean of 5,702 m (Table 4b). Considering glacier median elevation as a coarse approximation of glacier equilibrium line altitude (ELA), our results are in agreement with Benn and Owen (2005), who documented higher ELAs on the northern slopes of the Himalaya (6,000 – 6,200 m) compared to ELAs on the southern slopes (4,600 – 5,600 m). In our study area, we note a strong north - south gradient in glacier elevations, with glacier termini and median elevations much higher on northern side of the divide (China) compared to the southern side (Nepal and Sikkim) (+700 m and +400 m respectively). These differences seem to be consistent with general air circulation patterns in the area. The Asian summer monsoon brings large amounts of precipitation on the southern slopes of the Himalaya, favoring glacier growth at lower elevations and a lower ELA. In contrast, in the upper reaches of the valleys and on the Tibetan plateau, the monsoon is blocked by the topographic barrier (Clift and Plumb 2008),

causing a drier climate and higher glacier ELAs. There is also a slight east-west gradient in glacier elevations, with higher glacier minimum and median elevations on the western side (Nepal) (+50 m) compared to the eastern side (Sikkim). This can be explained by the location of Nepalese glaciers on the western side of the topographic divide, away from the prevailing monsoon, but this gradient is less pronounced.

The average slope of all glaciers in spatial domain 1 was 23 degrees, with a positive skew (skewness = 0.38) (Fig. 4b) and no significant differences among the four regions ($p > 0.05$) (Table 4b). Similar values for average glacier slopes (22 degrees) were reported for the Khumbu region in Nepal (Salerno et al. 2008; Bajracharya and Shrestha 2011), indicating a general tendency for steep glaciers in this area. Glacier length ranged from 0.08 km to 23 km (Zemu glacier), with an average of 2 km (Fig. 4c). For Zemu, Mool (2002) reported a length of 26 km in 1970's, and the Geologic Survey of India (Sangewar and Shukla 2009) reported 28 km for the same glacier based on 1970 topographic maps, suggesting a decrease in length in the last 30 years. Glacier thickness ranged from 3 m to 144 m, with the highest frequency for thicknesses less than 30 m (Fig. 4d). The frequency distribution of both glacier length and thickness were positively skewed, with long tails, indicating the prevalence of short, shallow valley-type glaciers. Glacier aspect shows two predominant orientations: west-northwest (W-NW) and east-northeast (E-NE), following the topographic divide (Fig. 5). On average, glaciers on the Nepal side had an average aspect of 237 degrees (SW), whereas glaciers on the Sikkim side had an average aspect of 131 degrees (SE), consistent with local topography. The predominant orientation of glaciers southwards, in the direction of the prevailing monsoon circulation was noted in other studies in the area, notably the Khumbu region (average aspect 181 degrees) (Mool et al. 2002; Salerno et al. 2008).

[Fig. 5]

A comparison between clean and debris-covered glaciers (two sample F-test for variances) showed significant differences in terms of glacier area, area change, minimum elevation, altitudinal range and length ($p < 0.05$) (Table 5). Clean glaciers in this area are ~10 times smaller (2 km^2 on average) than debris-covered glaciers (23 km^2), they have higher termini elevations (+ 535 m), and an overall altitudinal range about 3 times smaller than debris-covered glaciers (Table 5). These topographic differences might play an important role in determining a glacier's response to climate forcing, and will be discussed in the context of area changes (section 5).

[Table 5]

4.2 Glacier area changes 1962 - 2006 (spatial domain 2)

For the 50 glaciers in eastern Nepal (Tamor basin) and Sikkim (Zemu basin), the mean glacier elevation was 5634 m, mean maximum elevation was 6447 m, and 21 % of the glacierized area was covered by debris. We note that in this subset area, there is a higher percentage of debris than the entire spatial domain (11%), due to the exclusion of small, clean glaciers in China and Bhutan. The overall glacier surface area change from 1962 (Corona) to 2006 (QuickBird) was -10.3% (-0.24 ±0.08% yr^{-1}) (Table 6). On a glacier-by-glacier basis, glaciers lost 0.7% to 64 % of their area, with a mean of 25% (0.56 % yr^{-1}) from 1962 to 2006 (Fig. 6). The spatial distribution of these area changes, illustrated in Fig. 6, shows that the largest area changes (> 50% area loss) occurred only for a few isolated glaciers in the northern and southern extremities of the study area. A closer examination of these glaciers revealed that these were small glaciers (< 1 km^2), with steep slopes (mean of 25 degrees), little debris cover (< 6% of glacier area on average), and lower termini elevations than the entire study area (4,423 m for spatial domain 1).

[Table 6 and Fig. 6]

We note some differences between clean and debris-covered glaciers in terms of glacier-by-glacier area changes. Clean glaciers lost 3.4 to 64% of their area, with a mean of 32.6%, while debris-covered glaciers lost only 0.7% to 61% of their area, with a mean of 14.3 %. The difference in mean rates of area change between clean and debris covered glaciers was statistically significant based on two-sample F-test (p-value < 0.05). On Fig. 7a-b, we show a larger spread and a higher percentage of surface area loss of clean glaciers compared to debris-covered glaciers. For both glacier types, however, there is a high variability in percent area change, perhaps due to other factors such as local topography.

[Fig. 7 a-b]

The percent area change per glacier was negatively correlated to glacier maximum elevation, altitudinal range, median elevation, glacier area, percent debris cover, aspect and precipitation (correlation significant at 90% confidence interval, $p<0.1$) (Table 7). Of these, the strongest correlation was found for maximum elevation and altitudinal range, indicating that glaciers located on lower summits, with a small altitudinal range experienced larger area loss. The geographic location of glaciers (latitude and longitude), slope, solar radiation and minimum elevations were not statistically significant (Table 7).

[Table 7]

The percent of debris cover was negatively correlated to the percent area change, with a weak but significant correlation ($r = -0.25$; $p<0.05$, confidence interval 95%), indicating that glaciers with larger extents of debris cover tend to lose less area than clean glaciers.

5. *Discussion*

5.1 Glacier area changes and accuracy

The rates of surface area loss of -0.24 ± 0.08% yr^{-1} from 1962 to 2006, presented above, are in agreement with other studies from the southern slopes of the Himalaya. Similar rates of area change (-0.1 to -0.3% yr^{-1}) were reported from Khumbu and Garwhal regions,

west of our study area, for approximately the same time period (Bolch et al. 2008a; Bhambri et al. 2011; Nuimura et al. 2012; Basnett et al. 2013; Thakuri et al. 2014). Similarly, for glaciers of Bhutan, east of our study area, Karma et al. (2003) found an average surface glacier area change of -0.3% yr^{-1} from 1963 to 1993. It is worth mentioning that these rates of area loss are lower than those previously reported for the drier monsoon-transition zone in the western Himalaya (0.7% yr^{-1}) by Kulkarni et al. (2007), which raised concerns about the future of Himalayan glaciers. In a more recent study, Bahuguna et al. (2014) found lower rates of glacier area loss of about 0.4% yr^{-1} for the same area (Himachal Pradesh in the western Himalaya), which is in agreement with rates of area loss we report here for eastern part. Glacier area changes have been updated in more recent studies (Bolch et al. 2012; Bahuguna et al. 2014; Racoviteanu et al. 2014), and overall these findings are pointing at lower rates of area loss than previously reported, particularly in the Indian Himalaya.

Inconsistencies in glacier area change estimates have been pointed out in other studies, for the Himalaya and elsewhere (Racoviteanu et al. 2008a; Racoviteanu et al. 2008b), and are also noted in the current study. Glacier area changes in the Himalaya are heterogenous, and depend on a variety of factors including local topography and climate, so some caution should be applied when comparing rates of area changes from one area to another areas, even in the same climatic zone. For example, for Sikkim, we estimated a surface area change of -88.9 ± 5 km^2 (-13.5% from 1962 to 2006, or -0.36 ± 0.17 % yr^{-1}). This area change is higher than the area change for the larger Kanchenjunga-Sikkim area (-0.24% yr^{-1}). Other studies in this area point to contrasting results. For the same geographic area, Basnett et al. (2013) reported an area change of -0.16 ± 0.10 % yr^{-1} from 1989/1990 to 2009/2010), which is much lower than our findings. In contrast, a recent study (Bahuguna et al. 2014) reported the highest rates of area change (about -0.8% yr^{-1}) for the last decade, even higher than rates reported previously for the western Himalaya by Kulkarni et al. (2007). We

speculate that such large differences might be due to errors inherent in the baseline datasets, coupled with misclassification due to snow cover or debris-covered areas.

The glacier area changes reported for Sikkim by various teams, using a variety of data including topograohic maps (Table 8), illustrates this point. For example, for Sikkim, our study estimated 569 km^2 ± 70 km^2 of glacierized area in 2000 based on Landsat/ASTER data (section 4.1). For the same time period, Mool et al. (2002) reported an area of 577 km^2 based on the same source imagery (Landsat ETM+) (Table 8). These two area estimates differ only by 8.2 km^2 (1.4%) of our estimated area, only the number of glacier differs substantially (186 glaciers in our study compared to 285 glaciers in ICIMOD study), most likely due to the way in which ice masses were split and how glaciers were counted. Methodology differences and inconsistencies in glacier estimates are quite common in multi-temporal image analysis performed by different analysts, and were previously noted in other areas of the world (Racoviteanu et al. 2009). Similarly, for the 1962 decade, our analysis of Corona 1962 imagery for Sikkim yielded 178 glaciers with an area of 658 ±20 km^2. In a recent publication (Racoviteanu et al. 2014), we reported 158 glaciers with an area of 742 km^2 for the 1960s based on the Swiss topographic map. The Geological Survey of India (GSI) (Sangewar and Shukla 2009) reported 449 glaciers with an area of 706 km^2 for the 1970s based on topographic maps. Our 1962 Corona glacier inventory yields a smaller total glacier area than the one based on the topographic map (84 km^2, or 11%) (Racoviteanu et al. 2014) or the GSI inventory based on topographic maps (48.3 km^2, or 7 % area) (Sangewar and Shukla 2009). We consider that both of these mentioned studies overestimated the glacier area in the 1960s, perhaps due to the presence of persistent snow in the source aerial imagery.

Subsequent glacier inventories in Sikkim also point to contradictory patterns. For the 1980s, another study (Kulkarni 1992b) reported a glacierized area of 431 km^2 for 1987/1989 based on Indian IRS-1A and Landsat data. Considering our 1962 Corona inventory, this

would imply an area loss of 42% since 1962 (2.1% yr^{-1}), followed by a strong increase in glacier area (+33.5 %, or +3% yr^{-1}) from 1987/1988 to 2000 (based on our Landsat analysis), which is undocumented in this area. We consider the 1987/89 estimates to be highly unreliable, given that there are no glacier surges that might induce an apparent "glacier growth". In some areas, we noted omissions of some debris-covered tongues from the glacier maps, which might explain some of the differences. We consider the Corona 1962 dataset to be more reliable than the inventories based on topographic maps, and hence we used this dataset as baseline for comparison with the recent imagery.

[Table 8 here]

5.2 Topographic and climatic controls on area changes

In this study, we found that topographic factors, more notably glacier altitude (maximum, median, altitudinal range), glacier size and percent of debris cover were most important in determining rates of glacier area loss. Higher glacier elevations and larger altitudinal ranges reduced the rates of area loss, as was also noted in the Khumbu region in Nepal and elsewhere (Bolch et al. 2008a; Scherler et al. 2011; Loibl et al. 2014; Thakuri et al. 2014). The dependency of area change on glacier size and elevation is also consistent with observations from the Cordillera Blanca of Peru (Racoviteanu et al. 2008a) in the outer tropics, indicating consistent patterns in glacier area changes worldwide.

Glacier size plays a significant but less important role in determining area change, i.e. smaller glaciers experienced higher rates of area loss. In this study, the negative correlation between glacier size and area loss was statistically significant ($p<0.01$) (Table 7). The tendency of larger glaciers to lose less area (>20 km^2) was observed in various studies (Racoviteanu et al. 2008a; Salerno et al. 2008; Loibl et al. 2014), though in the case of Salerno et al. (2008), for the Khumbu, the correlation was not statistically significant. Glacier slope also plays a significant role in determining rates of area change ($p<0.01$), i.e. the

steeper the glacier, the larger the area loss observed in our study. The same tendency was observed in the Khumbu area (Salerno et al. 2008), but in our study the correlation was not significant, most likely because we included the ablation areas of glaciers. The presence of gentle slopes covered with supra-glacial debris in the ablation areas of glaciers, fairly common in this area, reduced the strength of the correlation.

Glacier aspect was a also found to be a control on area change, with more area loss for glaciers oriented southwards and south-west, but the correlation was not statistically significant ($p>0.01$). This is in agreement with findings from Salerno et al. (2008) for the Khumbu region, but is in contrast with results from Loibl et al. (2014) for the Nyainqêntanglha Range in southeastern Tibet, about 600 km east of our study area, who found that south-facing glaciers experienced smaller rates of terminus retreat.

Precipitation was also found significant in controlling glacier area loss, but the correlation was less strong than the glacier elevation factors mentioned above (Pearson's $r = -0.25$). In contrast, Loibl et al. (2014) showed that glaciers located in a monsoon-influenced area were more sensitive to climate change. This is in agreement with larger-scale studies (Gardelle et al. 2013), which indicated a tendency for enhanced glacier wastage in the eastern, monsoon-influenced parts of the Himalaya. With respect to climatic factors in this area, Basnett et al. (2013) reported an increase in mean annual temperature, more significantly in the winter (+2°C yr^{-1} in the last four decades). Increasing temperatures on the south slopes of the Himalayas were also noted in other studies (Shrestha et al. 2000; Thakuri et al. 2014) based on instrumental data, but were estimated to have less effect on glacier area than changes in precipitation because of the orientation of these glaciers towards the prevailing monsoon circulation. In our study, the climatic control on glacier area is not conclusive, and finer-resolution, more accurate temperature and precipitation datasets would be needed. Furthermore, similarly to areas further east (Loibl et al. 2014), average annual

solar radiation and latitude were not found to be significant controls on glacier area change in our study. Other factors such as supra-glacial debris cover might have a more important role than climate controls in preserving glacierized areas.

The impact of debris cover on reducing glacier area loss, noted in our study (Table 7) is in agreement with studies from Khumbu (Nuimura et al. 2012; Thakuri et al. 2014). Similarly to these studies, glaciers in our spatial domain 2 are located on the southern slopes of the Himalaya, which are heavily covered with debris cover due to the abundance of rock material from the steep slopes. In our study, glaciers have a slightly lower percent of debris cover (21%) compared to Khumbu area to the west (27 to 36%) (Bolch et al. 2008a; Scherler et al. 2011; Nuimura et al. 2012; Thakuri et al. 2014), but the rates of area change are similar (-0.2 to -0.3% yr^{-1}), indicating consistent glacier change patterns in this area of the Himalaya.

Similarly to the above-mentioned studies, we found that debris covered glaciers experienced smaller rates of surface area change from 1962 to 2006 (-14.3 % on average) compared to clean glaciers (-32.6% on average). The lower rates of glacier area loss of debris-covered tongues compared to clean glaciers may be partly due to their topographic characteristics (bigger size and larger altitudinal range compared to clean glaciers)(Table 5). Since these results are based on entire surface of the glaciers, however, the question remains whether debris-covered tongues have a distinct behavior from glaciers as a whole. Using only 14 selected debris-covered tongues, we found an area change of -3.8 km^2 (-3.4% or -0.07 % yr^{-1}) from 1962 to 2006. This is four times lower than the overall glacier area loss of 0.24% yr^{-1} in spatial domain 2. This result is consistent with previous studies in the central-eastern Himalaya (Bolch et al. 2008a; Bhambri et al. 2011; Thakuri et al. 2014), which reported lower rates of glacier surface area loss and stable or less retreating glacier termini for debris-covered tongues compared to clean glaciers (Scherler et al. 2011). Furthermore, debris covered glaciers may benefit from the insulating effect of debris cover above a certain

"critical" debris thickness (Mihalcea et al. 2008a; Zhang et al. 2011), which needs to be further investigated.

5.3 Surface temperature distribution on debris cover tongues

Surface characteristics of debris cover (thickness, thermal conductivity and resistance) may help explain the smaller rates of area change for the debris-covered ablation areas of glaciers. However, these are not easily available in this area due to the lack of field-based measurements, and the difficulty of conducting surveys on the debris-covered tongues. Therefore, in this study, we are qualitatively showing the distribution of surface temperature on selected debris-covered tongues in spatial domain 2 based on the 2002 ASTER scene. Fig. 8 shows a high variability in supra-glacial surface temperature at 90 m spatial resolution, but there is no clear general temperature trend for the eastern slopes (Sikkim side) versus the western slopes (Nepal) side. The fluctuations in surface temperatures along transects are clearly visible on Fig. 9, with some sharp spikes of high and low temperatures, particularly for Kanchenjunga and Yalung glaciers (labeled "A" and "B" on Fig. 8). This strong variability in supraglacier debris temperatures may be due to the presence of surface features such as debris thickness, size of the debris particles, and thermal resistance and conductivity of the debris. For the debris-covered tongues investigated here, the supraglacier temperatures range from 0ºC to 30ºC, suggesting that the supra-glacier debris heats up considerably during the day. At the glacier scale, temperature drops over supra-glacial features such as ice walls and supra-glacial lakes, which tend to be colder than the surrounding debris, and this is visible even at the coarse spatial resolution of the temperature data (90 m). On Fig. 9 we note the slight upward trend for supra-glacier temperature towards the glacier termini, particularly for Zemu glacier ("C" on Fig. 8). For this glacier, the middle-upper part of the debris surface is colder (-3 to 5ºC) than the last 10 km towards the glacier terminus (5 to 14ºC) (Fig. 9). In a different paper (Racoviteanu and Williams, 2012), we found similar patterns of surface

temperature increasing towards the glacier terminus for the same glacier, but based on a different scene (November 2001), indicating consistent patterns for this glacier. The higher surface temperatures towards the glacier terminus may indicate a thicker debris cover, which insulates the ice underneath, noted on other studies (Mihalcea et al. 2008a). The day-time debris temperature ranges and the strong spatial variability noted here are similar to the ones we found for Khumbu, west of this study area (-3 to 17ºC) (Racoviteanu et al. 2013b). In Khumbu, we found that supra-glacier debris had a distinct temperature signal compared to other surfaces such as non-ice moraine, clean ice, and supra-glacier/pro-glacier lakes, with more pronounced differences among these three during the daytime.

[Fig. 8 and 9]

The suitability of ASTER-based surface for inferring debris characteristics, most notably thickness, has been demonstrated in other studies (Suzuki et al. 2007; Mihalcea et al. 2008a; Zhang et al. 2011). For this study area, there were no field measurements available to test the validity of ASTER temperatures for quantifying supra-glacier debris characteristics. However, in a different study (Racoviteanu et al. 2013b), we validated ASTER-based surface temperatures extracted from 9 night scenes from 2010 – 2011 for the Khumbu by inverting field-based long-wave radiation (L_{out}) using the Stefan-Bolzmann law ($L_{out} = \varepsilon T^4$). The measurements were from the automatic weather station (AWS) installed on Changri Nup glacier (Wagnon et al. 2013). We found a good agreement between ASTER temperatures and field-based measurements ($R^2 = 0.92$) using a sensitivity analysis ($\varepsilon = 0.97 \pm 0.1$) to account for small-scale variability in emissivity. Given that the Kanchenjunga-Sikkim area has similar characteristics to Khumbu in terms of debris cover, geographic location, and that the images were acquired around the same time of the year as the Khumbu (Nov.- Jan.), we consider that this validation may be applicable to the present study area.

5.4 The role of glacier lakes

The role of supra-glacier/pro-glacier lakes for glacier area change in this area of the Himalaya was addressed in detail in recent studies (Basnett et al. 2013; Bajracharya et al. 2014). Gardelle et al. (2011) also pointed out the increased formation of supra-glacier lakes particularly for the eastern part of the Himalaya. A quantitative assessment of lake formation is beyond the scope of this paper; here we only illustrate qualitatively some of the changes occurring on glaciers with supra-glacial or pro-glacial lakes using high-resolution Corona and QuickBird imagery. For the Tista basin in Sikkim, Mool and Bajracharya (2003) inventoried 266 glacier lakes covering a total area of 20 km^2 (3.5% of the glacierized area) based on 2000 Landsat ETM+ imagery. For spatial domain 2, we estimated that glacier lakes covered 1.3% of the total debris-covered glacier area, or 5.8% of the area if we consider only the debris-cover (ablation) part, based on the QB/WV2 imagery. Salerno et al. (2012) reported similar percentage for the area of supraglacial lakes, i.e. (0.3 – 2% of the overall glacierized area) for the Khumbu region. While supra-glacier lakes do not cover extensive areas of the glacierized surface, they were shown to increase surface ablation rates in this part of the Himalaya (Sakai et al. 2002; Fujita and Sakai 2014). It was also shown that supra-glacier lakes located at the glacier terminus tend to merge to create large, fast growing pro-glacier lakes which accelerate glacier area loss (Basnett et al. 2013; Bajracharya et al. 2014).

Some of the pro-glacier lakes in our study area are visible on Fig. 10 and 11 for the northern part of spatial domain 2 (Changsang, East Langpo, Jongsang, Middle Lhonak, South Lhonak). Most of these lakes are moraine-dammed lakes, considered dangerous for potentially inducing glacier lake outburst flood events, and were shown to accelerate the glacier area loss in the recent decades (Bajracharya et al. 2014). Fig.10 a-b shows the rapid growth of the pro-glacier lake on N. and S. Lhonak glaciers in Sikkim, also noted in Basnett et al. (2013). A closer look at a subset area (Fig. 11) shows the visible growth of a pro-glacial

lake for the adjacent N. Lhonak and S. Lhonak glaciers. We estimate that these two glaciers retreated ~650 m and 1.3 km from 1962 to 2006, respectively. Another branch of N. Lhonak glacier has wasted significantly by ~1.5 km from 1962 to 2006, and a glacier outlet is now clearly visible. The northern branch of Jongsang glacier was entirely covered by a supra-glacier lake in 2006, while another part shows less significant rates of terminus retreat (~100 m in 44 years). While our purpose here is not to present glacier length changes, we note that these estimates are in agreement with trends of glacier thinning and increased glacier lake formation reported in this area of the Himalaya previously (Gardelle et al. 2011; Kääb et al. 2012; Basnett et al. 2013).

[Fig. 10 and 11]

6. Summary and outlook

In this study we combined remote sensing data from various sensors to construct a new glacier inventory for the Kanchenjunga-Sikkim region in the eastern Himalaya. Based on 1962 Corona and 2006 QuickBird imagery, we found an overall negative glacier surface area change of 0.24±0.08% yr^{-1} since 1962, in agreement with those noted in other studies in the eastern Himalaya, most notably the Khumbu. The area change rates reported here are lower than the average rate of -0.7% yr^{-1} reported in other glacierized areas of the world such as the Alps (Kääb et al. 2002), the Tien Shan (Bolch 2007) and the Peruvian Andes (Racoviteanu et al. 2008a). Glaciers exhibit heterogeneous patterns of area change, depending on topographic and climatic factors, more notably glacier altitude (maximum, median, altitudinal range), glacier size and percent debris cover. Glacier area changes depend strongly on glacier size and elevation, which is consistent with other areas in the central-eastern Himalaya (Thakuri et al. 2014), or elsewhere, for example the outer tropics (Racoviteanu et al. 2008a). The

conclusions drawn with respect to spatial patterns in glacier charscteristics, glacier area loss, and their topographic and climatic dependency, include:

- Glacier area change (loss) of -0.24 % ± 0.08% yr^{-1} from 1962 to 2006, with higher rates of area loss for clean glaciers (-34.6%, or -0.7% yr^{-1}) compared to debris-covered glaciers (-14.3% or -0.3 yr^{-1});
- The amount of glacier area loss is partly influenced by a glacier's headwater elevation, altitudinal range, glacier area, debris cover, aspect and precipitation;
- The largest area loss was found for small, steep glaciers with a smaller altitudinal range and less debris cover;
- Some of the debris-covered glacier tongues were found to be relatively stable, with significantly smaller rates of area change (-0.07% yr-1) compared to the entire debris-covered glacier surface (-0.3 yr^{-1});
- Supra-glacial debris cover is prevalent on the southern slopes of the Himalaya (14% of the glacierized area) compared to northern slopes (2%)
- Supraglacial lakes constitute about 6% of the debris covered area, and some of these supra-glacial lakes have merged to form pro-glacial lakes;
- Overall, these findings support the conclusion that while Himalayan glaciers are undoubtedly undergoing negative area change, the rates of area loss noted in recent studies, including the present one (0.2 – 0.4% yr^{-1} since the 1960s) are lower than other glacierized areas worldwide (0.7% yr^{-1}).

The glacier area change estimates reported here are subject to uncertainties, most notably with respect to early topographic maps and declassified Corona imagery, therefore a considerable effort was given to minimizing errors by multiple re-iterations of the glacier outlines. The understanding of the spatial patterns of glacier changes in the current study is limited by: 1) a lack of a baseline elevation dataset for the 1960 to compute glacier elevation

changes from 1960s to 2000; 2) lack of field-based measurements to validate debris-cover mapping and surface temperature distribution. With respect to the latter, while surface temperature trends show a slight increase towards the terminus, suggesting a thicker debris cover, the supra-glacial surface temperatures are highly heterogonous and require additional investigation. A further improvement in the current study will be to include the supra-glacial and pro-glacial lakes as a determinant factor for the glacier area change, perhaps in a more sophisticated multi-variate regression model. The glacier datasets constructed in this study can be further utilized to understand the behavior of glaciers in this little-investigated area of the Himalaya, particularly with respect to spatial patterns of glacier melt, and the contribution of glaciers to water resources.

Acknowledgements

This research was funded by a NASA Earth System Sciences (ESS) fellowship (NNX06AF66H), a National Science Foundation doctoral dissertation improvement grant (NSF DDRI award BC 0728075), a CIRES research fellowship, and a graduate fellowship from CU-Boulder. A. Racoviteanu's post-doctoral research was funded by Centre National d'Etudes Spatiales (CNES), France. Participation of M. Williams was supported by the NSF-funded Niwot Ridge Long-Term Ecological Research (LTER) program and the USAID Cooperative Agreement AID-OAA-A-11–00045. ASTER imagery was obtained through the NASA-funded Global Land Ice Measurements from Space (GLIMS) project. We are grateful to Jonathan Taylor at University of California-Fullerton for facilitating access to high-resolution imagery through the NASA Appropriations Grant # NNA07CN68G.

References:

Ageta, Y. and Higuchi, K. (1984). "Estimation of Mass Balance Components of a Summer-Accumulation Type Glacier in the Nepal Himalaya." Geografiska Annaler Series a-Physical Geography **66**(3): 249-255.

Andermann, C., Bonnet, S. and Gloaguen, R. (2011). "Evaluation of precipitation data sets along the Himalayan front." Geochemistry, Geophysics, Geosystems **12**(7): Q07023. 10.1029/2011gc003513.

Andreassen, L. M., F. paul, A. kääb and J. e. hausberg (2008). "The new Landsat-derived glacier inventory for Jotunheimen, Norway, and deduced glacier changes since the 1930s." Cryosphere Discuss **2**: 299 - 339.

Bahuguna, I. M., A.V. Kulkarni, M. L. Arrawatia and D. G. Shresta (2001). Glacier Atlas of Tista Basin (Sikkim Himalaya). Ahmedabad, India**:** SAC/RESA/MWRGGLI/SN/16.

Bahuguna, I. M., B. P. Rathore1, Brahmbhatt, R., Sharma, M., Dhar, S., Randhawa, S. S., Kumar, K., Romshoo, S., Shah, R. D. and Ganjoo, R. K. (2014). "Are the Himalayan glaciers retreating?" Curr Sci **106**: 1008 - 1013.

Bajracharya, S. R., Maharjan, S. B. and Shresta, F. (2014). "The status and decadal change of glaciers in Bhutan from 1980's to 2010 based on the satellite data." Annals of Glaciology **55**(66): 159 - 166. doi: 10.3189/2014AoG66A125, 2014.

Bajracharya, S. R., Mool, P. K. and Shresta, A. (2007). Impact of climate change on Himalayan glaciers and glacial lakes. ICIMOD, Kathmandu, pp.

Bajracharya, S. R. and Shrestha, B., Eds. (2011). The status of glaciers in the Hindu-Kush Himalauan Region. Kathmandu, Nepal, International Centre for Integrated Mountain Development (ICIMOD). 127 pp.

Basnett, S., Kulkarni, A. and Bolch, T. (2013). "The influence of debris cover and glacial lakes on the recession of glaciers in Sikkim Himalaya, India." Journal of Glaciology **59**(218): 1035 - 1046.

Benn, D. and Owen, L. A. (2005). "Equilibrium-line altitudes of the Last Glacial Maximum for the Himalaya and Tibet: an assessment and evaluation of results." Quaternary Int **138 - 139**: 55 -58.

Benn, D. I. and Owen, L. A. (1998). "The role of the Indian summer monsoon and the mid-latitude westerlies in Himalayan glaciation: review and speculative discussion." Journal of the Geological Society **155**(2): 353-363.

Berthier, E., Arnaud, Y., Kumar, R., Ahmad, S., Wagnon, P. and Chevallier, P. (2007). "Remote sensing estimates of glacier mass balances in the Himachal Pradesh (Western Himalaya, India)." Remote Sensing of Environment **108**(3): 327 - 338.

Berthier, E., Arnaud, Y., Vincent, C. and Remy, F. (2006). "Biases of SRTM in high-mountain areas: Implications for the monitoring of glacier volume changes." Geoph Res Lett **33**(8): L08502. doi:08510.01029/ 02006GL025862.

Bhambri, R. and Bolch, T. (2009a). "Glacier mapping: a review with special reference to the Indian Himalayas." Progr Phys Geogr **33**(5): 672 - 702.

Bhambri, R., Bolch, T., Chaujar, R. K. and Kulshreshth, S. C. (2010). "Glacier changes in the Garhwal Himalayas, India during the last 40 years based on remote sensing data." Journal of Glaciology **54**(203): 543 - 556.

Bhambri, R., Bolch, T., Chaujar, R. K. and Kulshreshtha, S. C. (2011). "Glacier changes in the Garhwal Himalaya, India, from 1968 to 2006 based on remote sensing." Journal of Glaciology **57**(203): 543 - 556.

Bhatt, B. C. and Nakamura, K. (2005). "Charactieristics of Monsoon rainfall around the Himalayas revealed by TRMM precipitation radar." Monthly Weather Review **133**: 149 - 165. http://dx.doi.org/10.1175/MWR-2846.1.

Bolch, T. (2007). "Climate change and glacier retreat in northern Tien Shan (Kazakhstan/Kyrgyzstan) using remote sensing data." Global Planet Change **56**(1-2): 1-12.

Bolch, T., Buchroithner, M. F., Pieczonka, T. and Kunert, A. (2008a). "Planimetric and Volumetric Glacier Changes in the Khumbu Himalaya since 1962 Using Corona, Landsat TM and ASTER Data." J Glaciol **54**(187): 592 - 600.

Bolch, T., Kulkarni, A., Kääb, A., Huggel, C., Paul, F., Cogley, J. G., Frey, H., Kargel, J. S., Fujita, K., Scheel, M., Bajracharya, S. and Stoffel, M. (2012). "The State and Fate of Himalayan Glaciers." Science **336**(6079): 310-314. 10.1126/science.1215828.

Bolch, T., M.F.Buchroithner, J.Peters, M.Baessler and Bajracharya, S. (2008b). "Identification of glacier motion and potentially dangerous glacial lakes in the Mt. Everest region/Nepal using spaceborne imagery." Nat.Hazards Earth Syst. Sci **8**: 1329 - 1340.

Bolch, T., Menounos, B. and Wheate, R. (2010). "Landsat-based inventory of glaciers in western Canada, 1985–2005." Remote Sensing of Environment **114**(1): 127 - 137.

Bolch, T., Pieczonka, T. and Benn, D. I. (2011). "Multi-decadal mass loss of glaciers in the Everest area (Nepal Himalaya) derived from stereo imagery." The Cryosphere **5**(2): 349-358. 10.5194/tc-5-349-2011.

Bookhagen, B. and Burbank, D. W. (2006). "Topography, relief and TRMM-derived rainfall variations along the Himalaya." Geoph Res Lett **33**(L08405): doi::10.1029/2006gl026037.

Burrough, P. A. and Mcdonnel, R. A. (1998). Principles of Geographic Information Systems., Oxford University Press.

Cgiar-Csi (2004). "Void-filled seamless SRTM data V1." International Centre for Tropical Agriculture (CIAT), available from the CGIAR-CSI SRTM 90m Database: http://srtm.csi.cgiar.org and http://www.ambiotek.com/topoview. Last accessed: 2014-04-01.

Clift, P. D. and Plumb, R. A. (2008). The Asian Monsoon: Causes, History and Effects. New York, Cambridge University Press.

Congalton, R. G. (1991). "A review of assessing the accuracy of classifications of remotely sensed data." Rem Sens Environ **37**: 35 - 46.

Dashora, A., Lohani, B. and Malik, J. N. (2007). "A repository of Earth resource information-CORONA satellite programme." Current Science **92**(7): 926 - 932.

Digital_Globe (2007). "QuickBird Imagery Products- Product Guide. Revision 4.7.3." Last accessed: 08-15, 2011, from http://www.hatfieldgroup.com/UserFiles/File/GISRemoteSensing/ResellerInfo/QuickBird/QuickBird%20Imagery%20Products%20-%20Product%20Guide.pdf.

Dozier, J. (1989). "Spectral Signature of Alpine Snow Cover from the Landsat Thematic Mapper." Remote Sensing of Environment **28**: 9 -22.

Farinotti, D., Huss, M., Bauder, A. and Funk, M. (2009). "An estimate of the glacier ice volume in the Swiss Alps." Global and Planetary Change **68**: 225 - 231.

Foster, L. A., Brock, B. W., Cutler, M. E. J. and Diotri, F. (2012). "A physically based method for estimating supraglacial debris thickness from thermal band remote-sensing data." Journal of Glaciology **58**(210): 677 - 690.

Frey, H., Paul, F. and Strozzi, T. (2012). "Compilation of a glacier inventory for the western Himalayas from satellite data: methods, challenges, and results." Remote Sensing of Environment **124**(0): 832-843. http://dx.doi.org/10.1016/j.rse.2012.06.020.

Fujii, Y. and Higuchi, K. (1977). "Statistical analyses of the forms of the glaciers in Khumbu Himal." Seppyo **39**: 7 - 14.

Fujita, K. and Sakai, A. (2014). "Modelling runoff from a Himalayan debris-covered glacier." Hydrol Earth Syst Sci Discuss **11**: 2441 - 2482.

Fujita, K., Suzuki, R., Nuimura, T. and Sakai, A. (2008). "Performance of ASTER and SRTM DEMs, and their potential for assessing glacial lakes in the Lunana region, Bhutan Himalaya." J Glaciol **54**(185): 220 - 228.

Gardelle, J., Arnaud, Y. and Berthier, E. (2011). "Contrasted evolution of glacial lakes along the Hindu Kush Himalaya mountain range between 1990 and 2009." Global and Planetary Change **75**(1-2): 47 - 55. 10.1016/j.gloplacha.2010.10.003.

Gardelle, J., Berthier, E., Arnaud, Y. and Kaab, A. (2013). "Region-wide glacier mass balances over the Pamir-Karakoram-Himalaya during 1999-2011." The Cryosphere **7**(4): 1263 - 1286, doi:1210.5194/tc-1267-1263-2013.

Gardelle, J. E., Berthier, E. and Y.Arnaud (2012). "Impact of resolution and radar penetration on glacier elevation changed computed from DEM differencing." Journal of Glaciology **58**(208): 419 - 422.

Hall, D. K., G. Riggs, A. and Salomonson, V. V. (1995). "Development of methods for mapping global snow cover using moderate resolution imaging spectroradiometer data." Rem Sens Environ **54**: 127 - 140.

Huss, M. and Farinotti, D. (2011). "Distributed ice thickness and volume of all glaciers around the globe." Journal of Geophysical Research **117**(F4). DOI: 10.1029/2012JF002523.

Imd. (1980). Climatological tables 1951 - 1980. Government of India, Controller of Publication, New Delhi, pp.

Immerzeel, W., Van Beek, L. P. H. and Bierkens, M. F. P. (2010). "Climate Change Will Affect the Asian Water Towers." Science **328**(5984): 1382-1385. 10.1126/science.1183188.

Immerzeel, W. W., Beek, L. P. H. V., Konz, M., Shrestha, A. B. and Bierkens, M. F. P. (2012). "Hydrological response to climate change in a glacierized catchment in the Himalayas." Climatic Change **110**(DOI 10.1007/s10584-011-0143-4): 721 - 736.

Iwata, S., Aoki, T., Kadota, T., Seko, K. and Yamaguchi, S. (2000). Morphological evolution of the debris cover on Khumbu Glacier, Nepal, between 1978 and 1995. in: Debris-covered glaciers. M. Nakawo, C.F. Raymond and A. Fountain (Eds.), IAHS. **264:** 3 - 11,

Kääb, A., Berthier, E., Nuth, C., Gardelle, J. and Arnaud, Y. (2012). "Contrasting patterns of early twenty-first-century glacier mass change in the Himalayas." Nature **488**(7412): 495-498. http://www.nature.com/nature/journal/v488/n7412/abs/nature11324.html#supplementary-information.

Kääb, A., Paul, F., Maisch, M., Hoelzle, M. and Haeberli, W. (2002). "The new remote-sensing-derived Swiss glacier inventory: II. First results." Annals of Glaciology **34**: 362 - 366.

Kamp, U., Byrne, M. and Bolch, T. (2011). "Glacier fluctuations between 1975 and 2008 in the Greater Himalaya Range of Zanskar, southern Ladakh." Journal of Mountain Sciences **8**(3): 374 - 389.

Karma, Ageta, Y., Naito, N., Iwata, S. and Yabuki, H. (2003). "Glacier distribution in the Himalayas and glacier shrinkage from 1963 to 1993 in the Bhutan Himalayas." Bulletin of Glaciological Research **20**: 29 - 40.

Kaser, G., Grosshauser, M. and Marzeion, B. (2010). "Contribution potential of glaciers to water availability in different climate regimes." Proceedings of the National Academy of Sciences of the United States of America **107**(47): 20223-20227. Doi 10.1073/Pnas.1008162107.

Kayastha, R. B., Takeuchi, Y., Nakawo, M. and Ageta, Y. (2000). Practical prediction of ice melting beneath various thickness of debris cover on Khumbu Glacier, Nepal, using a positive degree-day factor. in: Debris-Covered Glaciers. C.F. Raymond, Nakawo, M., Fountain, A. (Eds.). Wallingford, UK, IAHS. **264:** 71 - 81,

Krishna, A. P. (2005). "Snow and glacier cover assessment in the high mountains of Sikkim Himalaya." Hydrological Processes **19**(12): 2375-2383.

Kulkarni, A. V. (1992b). "Glacier inventory in the Himalaya." Natural resources management -a new perspective, NNRMS **Bangalore**: pp. 474-478.

Kulkarni, A. V., Bahuguna, I. M., Rathore, B. P., Singh, S. K., Randhawa, S. S., Sood, R. K. and Dhar, S. (2007). "Glacial retreat in Himalaya using Indian Remote Sensing satellite data." Current Science **92**(1): 69-74.

Loibl, D. M., Lehmkuhl, F. and Grießinger, J. (2014). "Reconstructing glacier retreat since the Little Ice Age in SE Tibet by glacier mapping and equilibrium line altitude calculation." Geomorphology **214**: 22 - 39. doi:10.1016/j.geomorph.2014.03.018.

Manley, W. F. (2008). Geospatial inventory and analysis of glaciers: A case study for the eastern Alaska Range, in Glaciers of Alaska. in: Satellite Image Atlas of Glaciers of the World: USGS Professional Paper 1386-K. R. S. Williams, Jr., and Ferrigno, J. G. (Eds.),

Mason, L. E. (1954). Abode of Snow: A History of Himalayan Exploration and Mountaineering. Dutton, New York City.

Mihalcea, C., Mayer, C., Diolaiuti, G., D'agata, C., Smiraglia, C., Lambrecht, A., Vuillermoz, E. and Tartari, G. (2008a). "Spatial distribution of debris thickness and melting from remote-sensing and meteorological data, at debris-covered Baltoro glacier, Karakoram, Pakistan." Annals of Glaciology **48**(1): 49-57.

Mihalcea, C. E., Brock, B. W., Diolaiuti, G. A., D'agata, C., Citterio, M., Kirkbride, M. P., Cutler, M. and Smiraglia, C. (2008b). "Using ASTER satellite and ground-based surface temperature measurements to derive supraglacial debris cover and thickness patterns on Miage Glacier (Mont Blanc Massif, Italy)." Cold Regions Science and Technology **52**(3): 341 - 354. doi:10.1016/j.coldregions.2007.03.004.

Mool, P. K. and Bajracharya, S. R. (2003). Tista Basin, Sikkim Himalaya: Inventory of Glaciers and Glacial Lakes and the Identification of Potential Glacial Lake Outburst Floods

(GLOFs) Affected by Global Warming in the Mountains of Himalayan Region. International Center for Integrated Mountain Development, Kathmandu, Nepal, 145 pp.

Mool, P. K., Bajracharya, S. R., Joshi, S. P., Sakya, K. and Baidya, A. (2002). Inventory of Glaciers, Glacial Lakes and Glacial Lake Outburst Floods Monitoring and Early Warning Systems in the Hindu-Kush Himalayan region, Nepal, International Center for Integrated Mountain Development, Nepal.

Nandy, S. N., Dhyani, P. P. and Samal, P. K. (2006) "Resource Information database for the Indian Himalaya, ENVIS Monograph No. 3 http://gbpihedenvis.nic.in/HTML/monograph3/Contents.html." Last accessed: 2014-07-01.

Narama, C., Kääb, A., Kajiura, T. and Abdrakhmatov, K. (2007). "Spatial variability of recent glacier area and volume changes in Central Asia using Corona, Landsat, ASTER and ALOS optical satellite data." Geophys Res Abstr **9**(08178).

Nuimura, T., Fujita, K., Yamaguchi, S. and Sharma, R. R. (2012). "Elevation changes of glaciers revealed by multitemporal digital elevation models calibrated by GPS survey in the Khumbu region, Nepal Himalaya, 19922008." Journal of Glaciology **58**(210): 648-656.

Nuth, C. and Kääb, A. (2011). "Co-registration and bias corrections of satellite elevation data sets for quantifying glacier thickness change." The Cryosphere(5): 271 - 290.

Palazzi, E., Von Hardenberg, J. and Provenzale, A. (2013). "Precipitation in the Hindu-Kush Karakoram Himalaya: Observations and future scenarios." Journal of Geophysical Research: Atmospheres **118**(1): 85-100. 10.1029/2012jd018697.

Paterson, W. S. B. (1994). The Physics of Glaciers, 3rd ed. Oxford, Pergamon.

Paul, F., Barrand, N., Berthier, E., Bolch, T., Casey, K., Frey, H., Joshi, S. P., Konovalov, V., Bris, R. L., Mölg, N., Nosenko, G., Nuth, C., Pope, A., Racoviteanu, A., Rastner, P., Raup, B., Scharrer, K., Steffen, S. and Winsvold, S. (2013). "On the accuracy of glacier outlines derived from remote sensing data." Annals of Glaciology **54**(63). 10.3189/2013AoG63A296.

Pfeffer, W. T., Arendt, A. A., Bliss, A., Bolch, T., Cogley, J. G., Gardner, A. S., Hagen, J. O., Hock, R., Kaser, G., Kienholz, C., Miles, E. S., Moholdt, G., Mölg, N., Paul, F., Radić, V., Rastner, P., Raup, B. H., Rich, J., Sharp, M. J. and Randolph_Consortium (2014). "The Randolph Glacier Inventory: a globally complete inventory of glaciers." Journal of Glaciology **60**(221). doi: 10.3189/2014JoG13J176.

Racoviteanu, A., Armstrong, R. and Williams, M. (2013a). "Evaluation of an ice ablation model to estimate the contribution of melting glacier ice to annual discharge in the Nepal Himalaya." Water Resources Research **49**(9): 5117 - 5133. DOI: 10.1002/wrcr.20370.

Racoviteanu, A., Arnaud, Y., Baghuna, I. M., Bajracharya, S., Berthier, E., Bhambri, R., Bolch, T., Byrne, M., Chaujar, R. K., Kääb, A., Kamp, U., Kargel, J., Kulkarni, A. V., Leonard, G., Mool, P., Frauenfelder, R. and Sossna, I. (2014). Himalayan glaciers. in: Global Land and Ice Monitoring from Space: Satellite Multispectral Imaging of Glaciers. Jeffrey S. Kargel, Michael P. Bishop, Andreas Kääb and Bruce H. Raup (Eds.). Heidelberg, Springer-Praxis**:** 549 - 582, 978-3-540-79817-0, "10.1007/978-3-540-79818-7:" 10.1007/978-3-540-79818-7.

Racoviteanu, A., Arnaud, Y. and Williams, M. (2008a). "Decadal changes in glacier parameters in Cordillera Blanca, Peru derived from remote sensing." J Glaciol **54**(186): 499 - 510.

Racoviteanu, A., Nicholson, L. and Arnaud, Y. (2013b). Surface characteristics of debris-covered glacier tongues in the Khumbu Himalaya derived from remote sensing texture analysis. European Geophysical Union (EGU) Genrral Assembly. Vienna, Austria. **15:** 10174.

Racoviteanu, A., Paul, F., Raup, B., Khalsa, S. J. S. and Armstrong, R. (2009). "Challenges and recommendations in mapping of glacier prameters from space: results of the 2008 Global Land Ice Measurements frpom Space (GLIMS) workshop, Boulder, Colorado, USA." Annals of Glaciology **50**(53): 53 - 69.

Racoviteanu, A., Williams, M. W. and Barry, R. (2008b). "Optical remote sensing of glacier mass balance: a review with focus on the Himalaya." Sensors **Special issue: Remote sensing of the environment**(8): 3355 - 3383.

Racoviteanu, A. E. and Williams, M. W. (2012). "Decision tree and texture analysis for mapping debris-covered glaciers: a case study from Kangchenjunga, eastern Himalaya." Remote Sensing Special issue **4**(10): 3078-3109, doi:3010.3390/rs4103078.

Raj, K. B. G., Remya, S. N. and Kumar, K. V. (2013). "Remote sensing-based hazard assessment of glacial lakes in Sikkim Himalaya." Current Science **104**(3): 359 - 364.

Raup, B. H., Kääb, A., Kargel, J. S., Bishop, M. P., Hamilton, G., Lee, E., Paul, F., Rau, F., Soltesz, D., Khalsa, S. J. S., Beedle, M. and Helm, C. (2007). "Remote sensing and GIS technology in the Global Land Ice Measurements from Space (GLIMS) Project." Computers and Geosciences **33**: 104-125.

Raup, B. H. and Khalsa, S. J. S. (2007). "GLIMS Analysis tutorial." GLIMS. Last accessed: 04-01-2014, from http://www.glims.org/MapsAndDocs/assets/GLIMS_Analysis_Tutorial_a4.pdf.

Rees, W. G. (2003). Remote sensing of snow and ice, Taylor & Francis Group, Boca Raton FL.

Sakai, A. and Fujita, K. (2010). "Correspondence: Formation conditions of supraglacial lakes on debris covered glaciers in the Himalaya." Journal of Glaciology **56**(195): 177 - 181.

Sakai, A., Nakawo, M. and Fujita, K. (2002). "Distribution Characteristics and Energy Balance of Ice Cliffs on Debris-Covered Glaciers, Nepal Himalaya." Arctic Antartcic and Alpine Research **34**(1): 12 - 19.

Salerno, F., Buraschi, E., Bruccoleri, G., G.Tartari and C.Smiraglia (2008). "Glacier surface-area changes in Sagarmatha pational park, Nepal, in the second half of the 20th century, by comparison of historical maps." Jounal of glaciology **54**(187): 738 - 752.

Salerno, F., Thakuri, S., D'agata, C., Smiraglia, C., Manfredi, E. C., Viviano, G. and Tartari, G. (2012). "Glacial lake distribution in the Mount Everest region: Uncertainty of measurement and conditions of formation." Global and Planetary Change **92-93**: 30-39.

Sangewar, C. V. and Shukla, S. P., Eds. (2009). Inventory of Himalayan glaciers: A Contribution to the International Hydrological Programme. Calcutta, Geological Survey of India (GSI Special Publication 34): An updated edition. 594 pp.

Scherler, D., Bookhagen, B. and Strecker, M. R. (2011). "Spatially variable response of Himalayan glaciers to climate change affected by debris cover." Nature Geosci **4**(3): 156-159. http://www.nature.com/ngeo/journal/v4/n3/abs/ngeo1068.html#supplementary-information.

Shanker, R. (2001). Glaciological studies in India, a contribution from Glaciological Survey of India. . Symposium on snow, ice and glacier, March 1999, Geological Survey of India Special Publication. 53, 11 - 15.

Shrestha, A., C.P.Wake, Dibb, J. E. and Mayevski, P. A. (2000). "Precipitation fluctuations in the Nepal Himalaya and its vicinity and relationship with some large-scale climatologic patterns." Int J Climatol **20**: 317 - 327.

Srikantia, S. V. (2000). "Restriction on maps: A denial of valid geographic information." Current Science **79**(4): 484 - 488.

Survey_of_India (2005). "National Map Policy." Survey of India. Last accessed: 2014 - 06 - 01, 2014, from http://www.surveyofindia.gov.in/tenders/nationalmappolicy/nationalmappolicy.pdf.

Thakuri, S., Salerno, F., C.Smiraglia, T.Bolch, D'agata, C., G.Viviano and Tartari, G. (2014). "Tracing glacier changes since the 1960s on the south slope of Mt. Everest (central Southern Himalaya) using optical satellite imagery." The Cryosphere **8**: 1297 - 1315. doi:10.5194/tc-8-1297-2014.

Usgs-Eros (1996). "USGS Declassified Imagery-1 ". Last accessed: 03-01, 2012, from http://eros.usgs.gov/#/Guides/disp1.

Wagnon, P., Vincent, C., Arnaud, Y., Berthier, E., Vuillermoz, E., Gruber, S., Ménégoz, M., Gilbert, A., Dumont, M. and Pokharel, B. (2013). "Seasonal and annual mass balances of Mera and Pokalde glaciers (Nepal Himalaya) since 2007." The Cryosphere.

Wessels, R. L., Kargel, J. S. and Kieffer, H. H. (2002). ASTER measurement of supraglacial lakes in the Mount Everest region of the Himalaya. in: Annals of Glaciology, Vol 34, 2002(Eds.). **34:** 399-408,

Yanai, M., Li, C. and Z.Song (1992). "Seasonal heating of the Tibetan plateau and its effect on the evolution of the Asian summer monsoon." J. Meteorol. Soc. Jpn **70**: 319 - 351.

Zhang, Y., Fujita, K., Liu, S., Liu, Q. and Nuimura, T. (2011). "Distribution of debris thickness and its effect on ice melt at Hailuogou glacier, southeastern Tibetan Plateau, using in situ surveys and ASTER imagery." Journal of Glaciology **57**(206): 1147-1157.

Tables

Table 1. Summary of satellite imagery used in this study

Sensor	Scene ID	Date	Spatial resolution	Image type
Corona KH4	DS009048070DA244 DS009048070DA243 DS009048070DA242	1962-10-25	7.5 m	Panchromatic
Landsat ETM+	L7CPF20001001_20001231_07	2000-12-26	15 m 28.5 m 90 m	Pancromatic Visible,shortwave Thermal infrared
ASTER	AST_L1A#003_12012000051205_07292001131755	2000-12-01	15 m 30 m 90 m	Visible Shortwave Thermal infrared
	AST_L1A#003_12012000051214_07292001131813	2000-12-01		
	AST_L1A_00311272001045729_02222004173619	2001-11-27		
	AST_L1A#00301052002050207_01302002193030	2002-01-05		
	AST_L1A#00301052002050216_01302002193046	2002-01-05		
	AST_08_00310292002045428_20101212181710_16443	2002-10-29	90 m	Surface kinetic temperature
QuickBird	1010010004BD8700 1010010004BB8F00	2006-01-01 2006-01-06	2.4 m	Visible, shortwave
WorldView -2	102001000FBA1D00 102001000586E700	2010-12-02 2009-12-01	.50 m	Panchromatic

Table 2. Spatial domains used for analysis and their characteristics

Spatial domain	Number of glaciers	Details
1	487	The entire area of the Eastern Himalaya, in this study extending from Sikkim to China, as well as parts of W Bhutan and E Nepal.
2	50	Parts of Sikkim (Tista basin) and Nepal (Tamor basin)

Table 3. Topographic zones in spatial domain 1

	N side (China)	W side (Nepal)	E side (Sikkim)	E side (Bhutan)
Mean basin elevation (m)	4931	4819	4658	4491
Mean rainfall TRMM (mm/yr)	146	805	977	383

Table 4. Topographic parameters for glaciers in spatial domain 1 and sub-regions based on 2000s Landsat/ASTER analysis. All parameters are presented on a) region-by-region and b) glacier-by-glacier basis from the SRTM DEM. Debris cover fraction is calculated as % glacier area of debris covered glaciers only.

Parameter	All	Nepal	Sikkim	Bhutan	China
a) Region-wide averages					
Number of glaciers	487	162	186	30	109
Glacierized area (km^2)	1463 ± 88	488 ± 29	569±34	106 ± 6	300±18
Number of debris-covered tongues	68	30	27	7	4
Debris cover area (km^2)	161±10	64±4	78±5	14±1	6±0.4
Debris cover (% total glacier area)	11	13	14	13	2
b) Glacier averages					
Minimum elevation (m)	4908	4760	4702	4926	5425
Median elevation (m)	5702	5715	5569	5652	5950
Maximum elevation (m)	6793	6928	6908	6685	6530
Slope (degree)	23	24	23	27	21
Aspect (degree)	177	236	131	134	180
Mean glacier size (km^2)	3	3	3	4	3
Length (km)	2	2	2	3	2
Thickness (m)	24	23	23	31	27
Debris cover fraction (%)	23	21	23	32	17

Table 5. Comparison of glacier parameters for clean glaciers versus debris-covered glaciers.

Parameter	**Clean glaciers**	**Debris-covered glaciers**
Area (km^2)	2	23
Area change (%)	31	14
Slope	24	25
Minimum elevation (m)	5240	4704
Median elevation (m)	5625	5645
Altitudinal range (m)	777	2339
Length (km)	2	8

Table 6. Glacier area changes for the 50 glaciers in spatial domain 2, from 1962 to 2006.

Data source	**Area (km^2)**	**Area change since 1962 (% yr^{-1})**
1962 Corona	599±18	
2000 Landsat/ASTER	551±34	-0.20 +/-0.16
2006 QuickBird	537±8	-0.24 +/-0.08

Table 7 Correlations between area change and topographic and climatic variables, arranged in order of strength of correlation.

Regression	Pearson's r	P-value
Maximum elevation	-0.63	<0.01**
Altitudinal range	-0.58	<0.01**
Median elevation	-0.47	<0.01**
Glacier size	-0.41	<0.01**
Precipitation	-0.39	<0.01**
Minimum elevation	0.26	>0.1
Percent debris	-0.25	<0.01
Solar radiation	0.17	>0.1
Slope	0.14	>0.1
Latitude	-0.06	>0.1
Longitude	0.06	>0.1
Aspect	0.04	<0.01**

** Correlation is significant at the 0.01 level (2-tailed).

Table 8 Glacier area change in Sikkim based on previous studies. The percent area change is given with respect to the 1962 Corona glacier inventory from this study.

Study	Year	Data source	Number of glaciers	Area (km^2)	Area change since 1960s	
					%	% yr^{-1}
This study	1962	Corona KH4	178	658±20	-	-
Geological Survey of India (1999)	~1960 -1970s	Indian 1:63,000 topographic maps	449	706	+7.3	+0.9
Kulkarni and Narain (1990)	1987/ 1989	IRS-1C satellite images	n/a	426	-35.0	-1.4
ICIMOD Mool et al, (2002)	2000	Landsat TM, IRS-1C, topographic maps	285	577	-11.4	-0.3
This study	2000	Landsat TM, ASTER	185	569 ±34	13.5 ±6.4	0.3 ±0.1

List of figures

Fig. 5 Aspect frequency distribution of the 487 glaciers in spatial domain 1 based on Landsat/ASTER analysis. On average, glaciers in this area are preferentially oriented towards NW (300°) and NE (60°).

Fig. 6 Spatial patterns in glacier area change derived from 1962 Corona and 2006 QB data.

Fig. 7 Dependency of glacier area change 1962 – 2000 on a) glacier altitudinal range (maximum – minimum elevation) and b) glacier area. Debris-covered glaciers are shown as grey solid circles; clean glaciers are shown as black solid triangles.

Fig. 8 Distribution of surface temperatures along longitudinal for selected debris-covered tongues in spatial domain 2. Temperatures are extracted from ASTER kinetic temperature data (AST08) from the Oct 29th, 2002 image.

Fig. 9 Surface temperature distribution along longitudinal transects from selected glaciers. Distance is measured from the upper part of the debris-covered area down glacier to the terminus. Labels point to: A- Kanchenjunga glacier, B- Yalung glacier and C- Zemu glacier.

Fig. 10 Area changes for some glaciers in the Zema Chhu basin Sikkim from 1962 to 2006: a) 1962 Corona-based glacier outlines (in blue) and b) 2006 QB glacier outlines (in orange).

Fig. 11 Close-up view of glacier area changes around the N. and S. Lhonak glaciers 1962 to 2006, showing changes in the pro-glacial lakes.

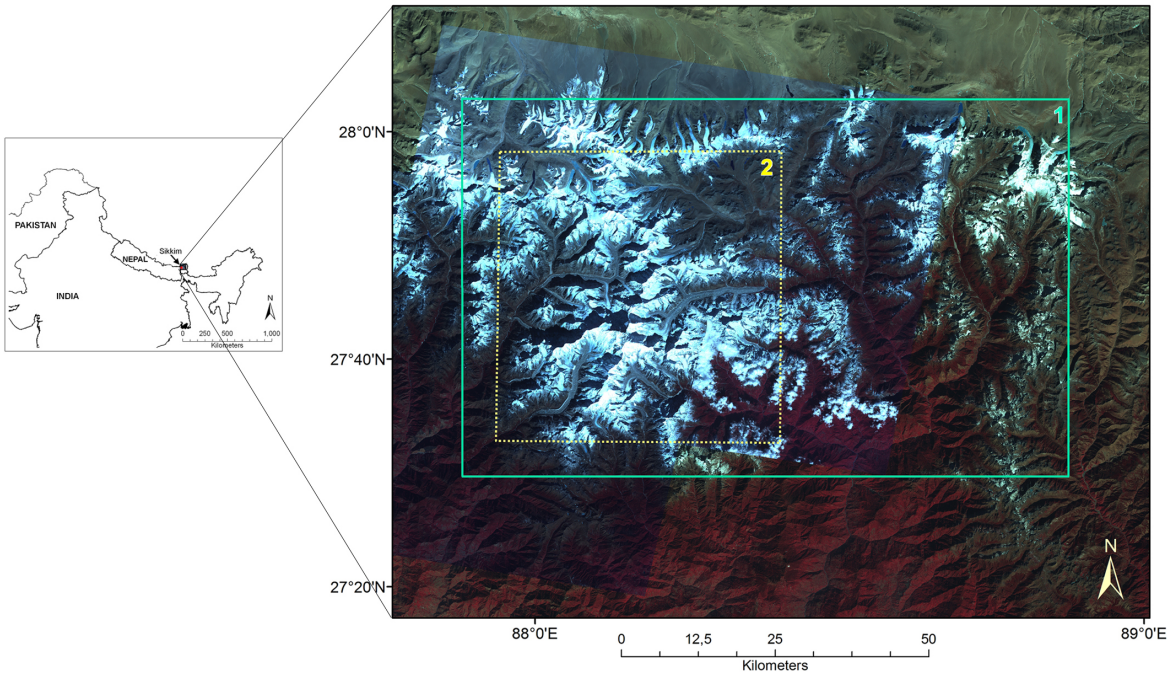
PAKISTAN
NEPAL
Sikkim
INDIA
N
0 250 500 1,000
Kilometers
28°0'N
27°40'N
27°20'N
88°0'E
89°0'E
1
2
N
0 12,5 25 50
Kilometers

Fig.1

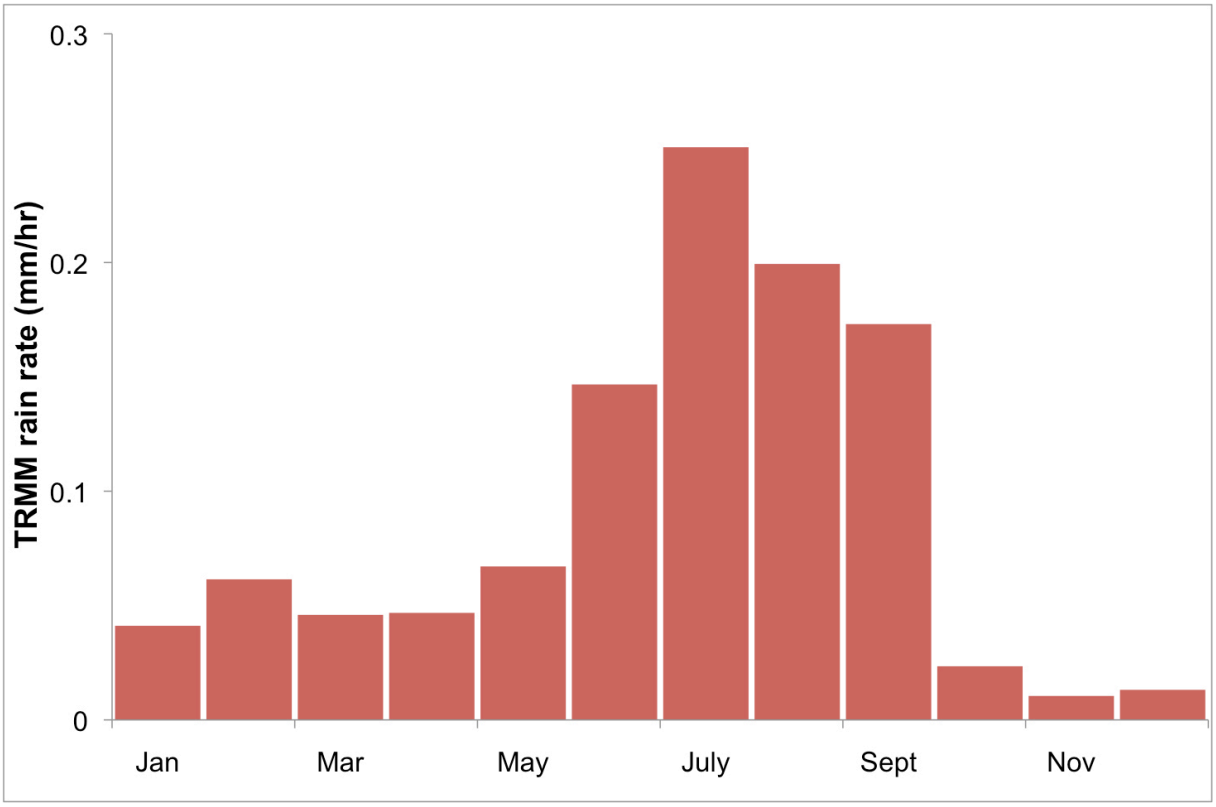

Fig. 2

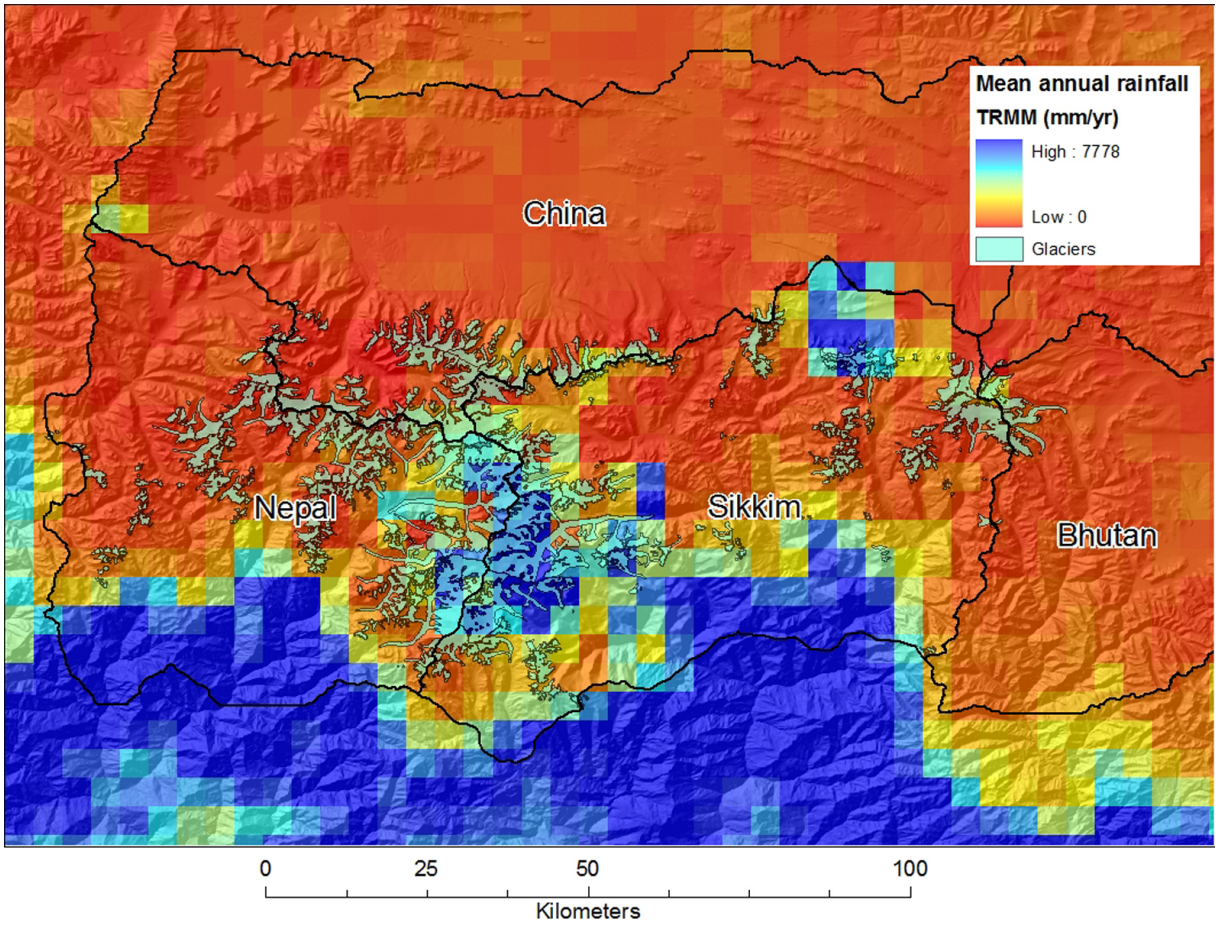
Mean annual rainfall
TRMM (mm/yr)
High : 7778
Low : 0
Glaciers
China
Nepal
Sikkim
Bhutan
0
25
50
100
Kilometers

Fig.3

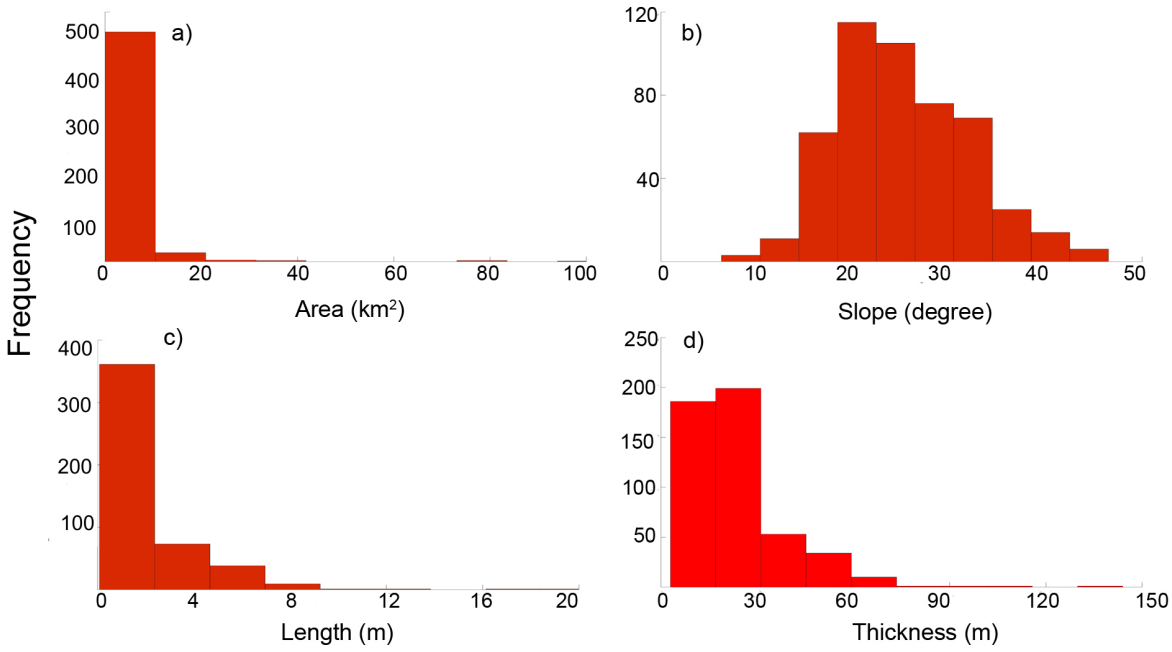
a)
b)
c)
d)
Frequency
Area (km²)
Slope (degree)
Length (m)
Thickness (m)
500
400
300
200
100
0
20
40
60
80
100
120
80
40
0
10
20
30
40
50
400
300
200
100
0
4
8
12
16
20
250
200
150
100
50
0
30
60
90
120
150

Fig. 4

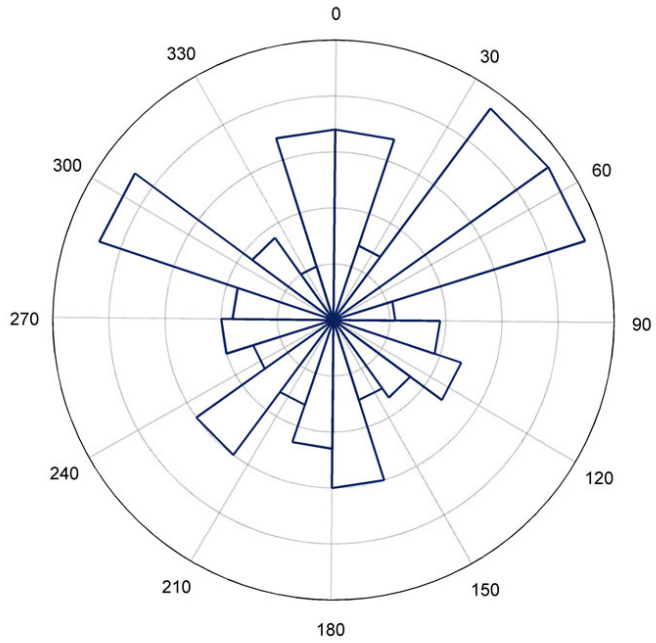

Fig. 5

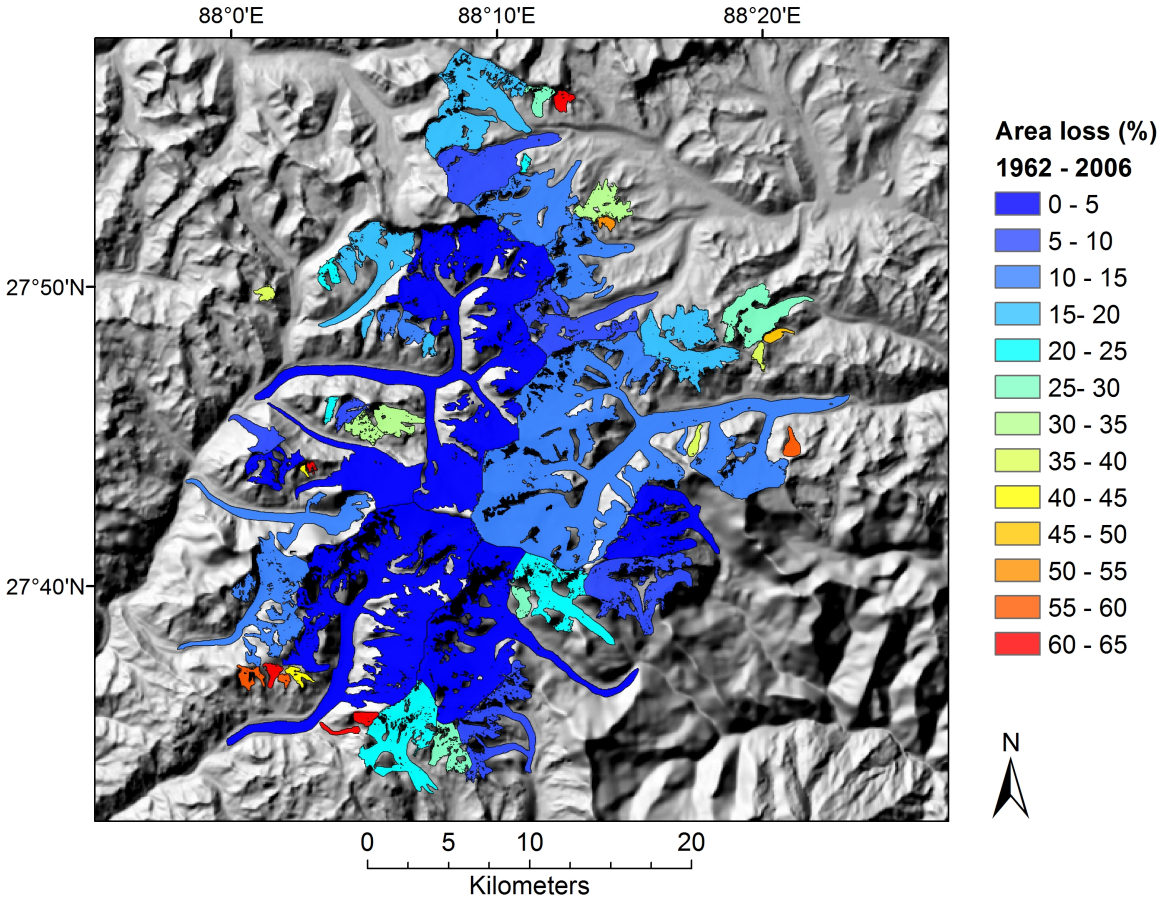
88°0'E
88°10'E
88°20'E
27°50'N
27°40'N
Area loss (%)
1962 - 2006
0 - 5
5 - 10
10 - 15
15- 20
20 - 25
25- 30
30 - 35
35 - 40
40 - 45
45 - 50
50 - 55
55 - 60
60 - 65
N
0 5 10 20
Kilometers

Fig. 6

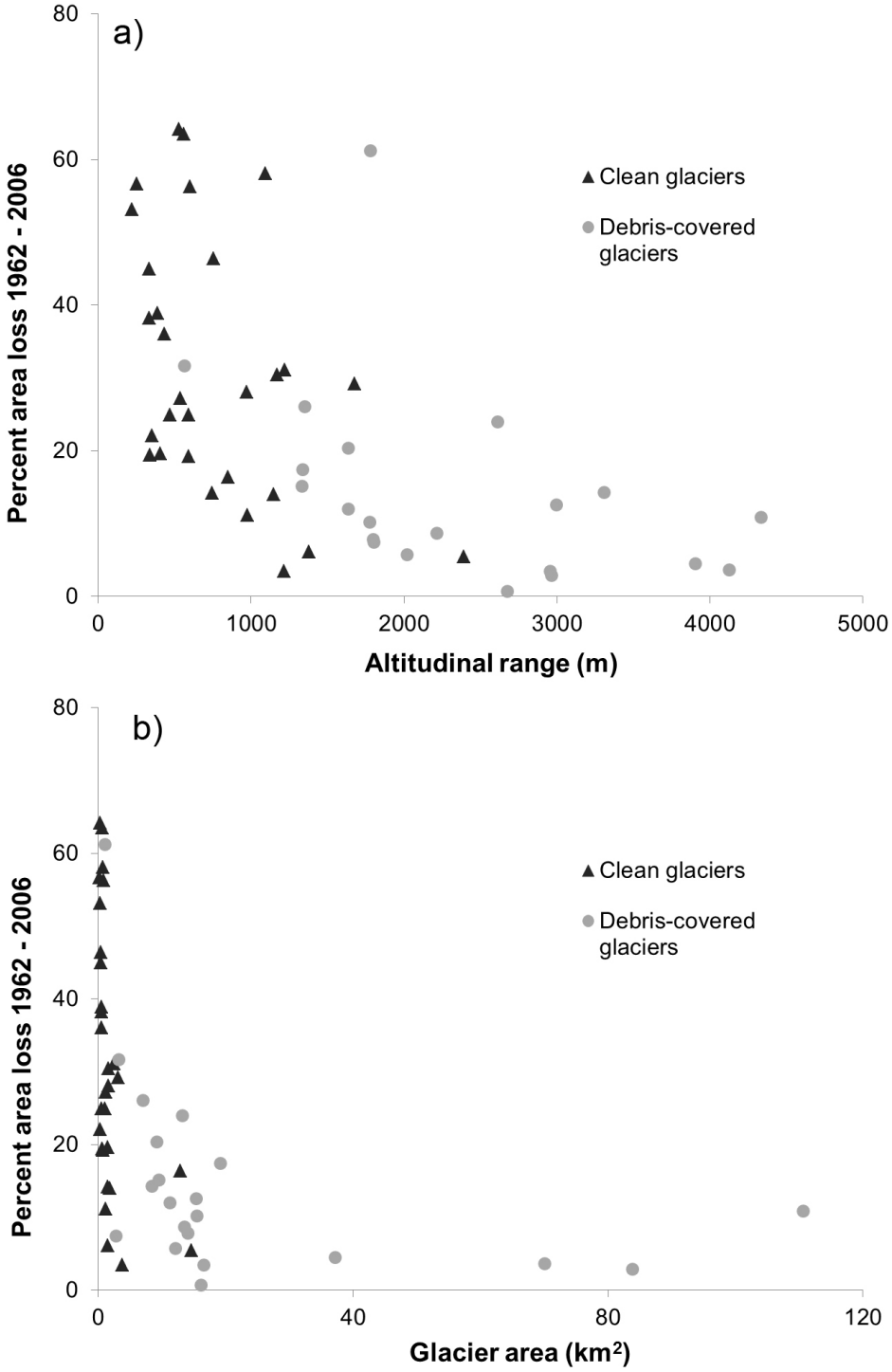
a)
Percent area loss 1962 - 2006
Altitudinal range (m)
Clean glaciers
Debris-covered glaciers
0
20
40
60
80
0
1000
2000
3000
4000
5000
b)
Percent area loss 1962 - 2006
Glacier area (km²)
Clean glaciers
Debris-covered glaciers
0
20
40
60
80
0
40
80
120

Fig. 7

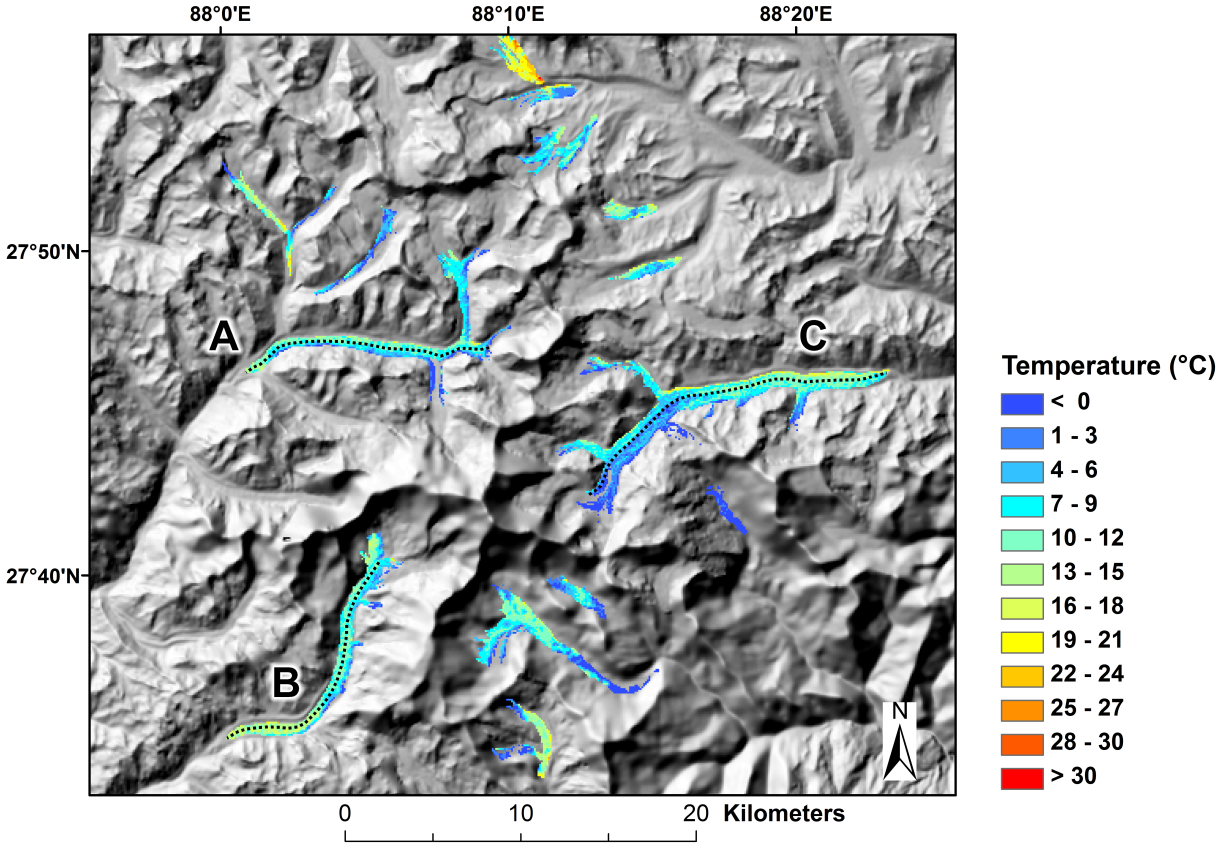
88°0'E
88°10'E
88°20'E
27°50'N
27°40'N
A
B
C
N
0
10
20
Kilometers
Temperature (°C)
< 0
1 - 3
4 - 6
7 - 9
10 - 12
13 - 15
16 - 18
19 - 21
22 - 24
25 - 27
28 - 30
> 30

Fig. 8

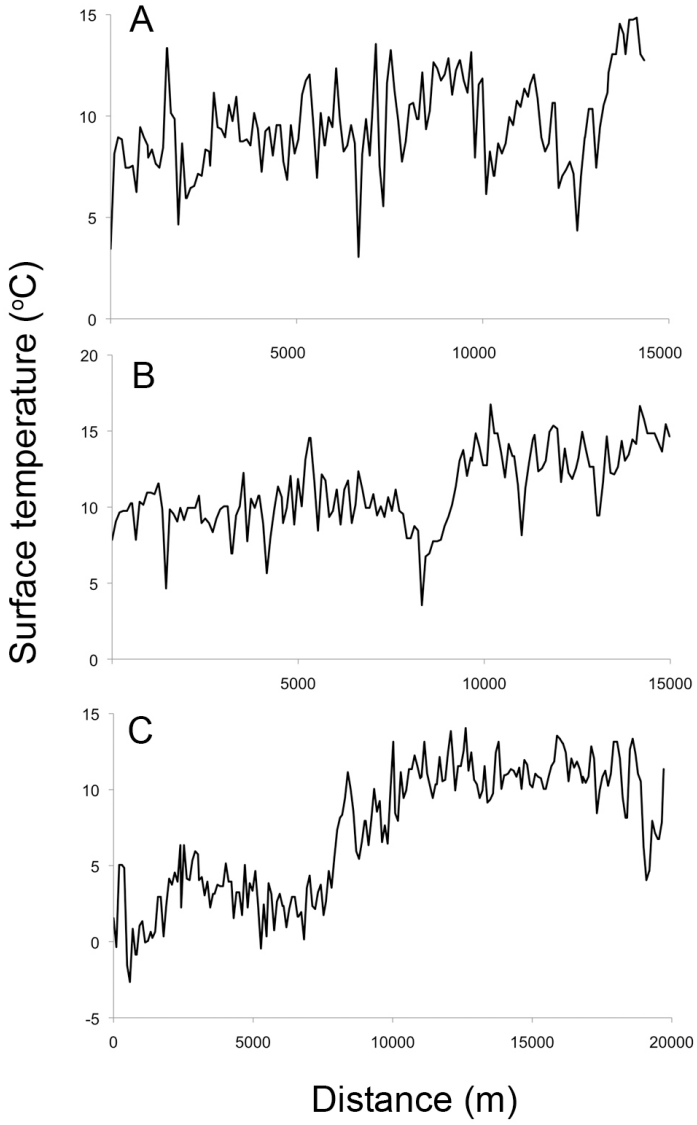
A
B
C
Surface temperature (°C)
Distance (m)
15
10
5
0
20
-5
5000
10000
15000
20000

Fig. 9

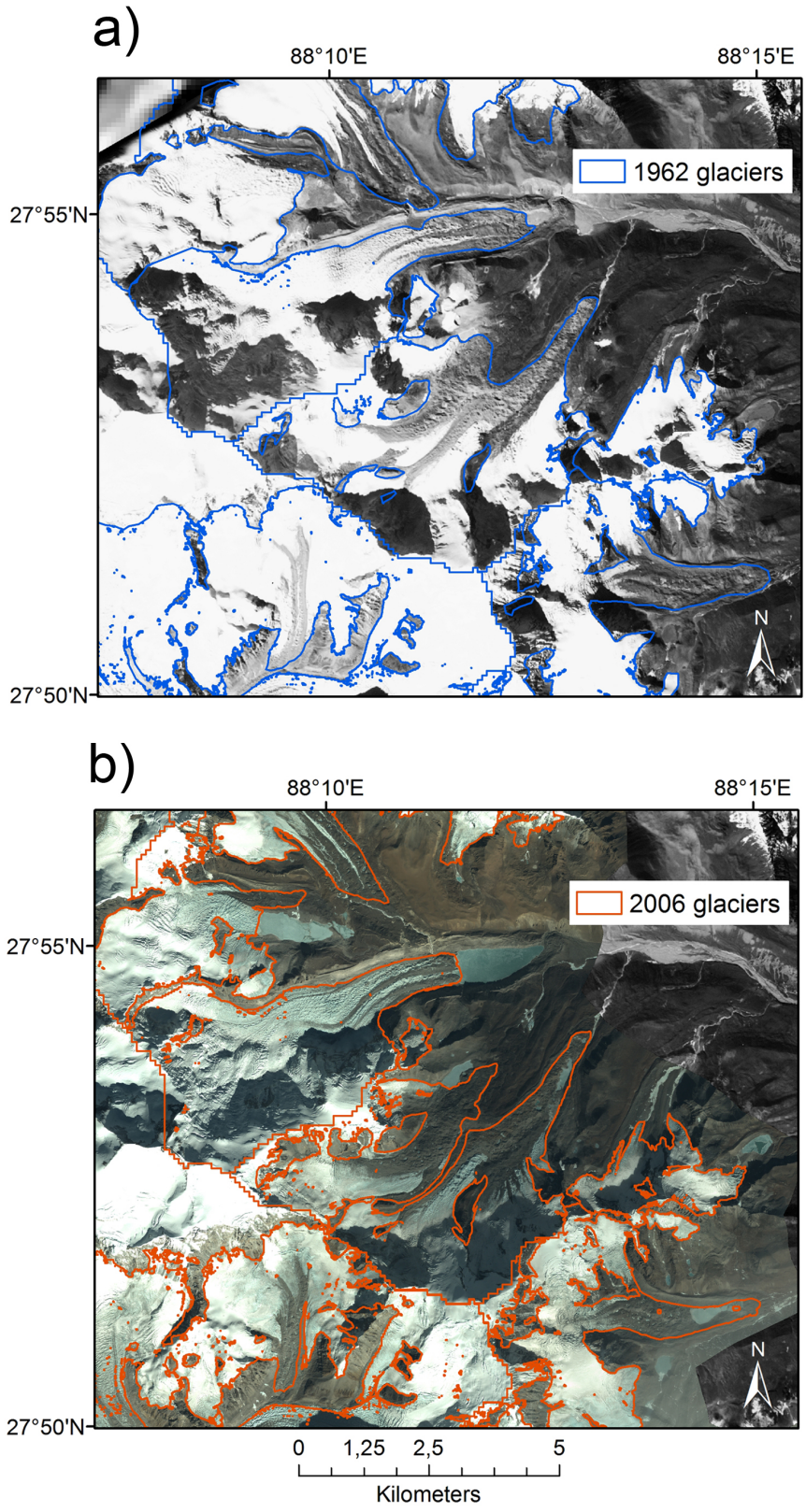
a)
88°10'E
88°15'E
27°55'N
27°50'N
1962 glaciers
N
b)
88°10'E
88°15'E
27°55'N
27°50'N
2006 glaciers
N
0
1,25
2,5
5
Kilometers

Fig. 10

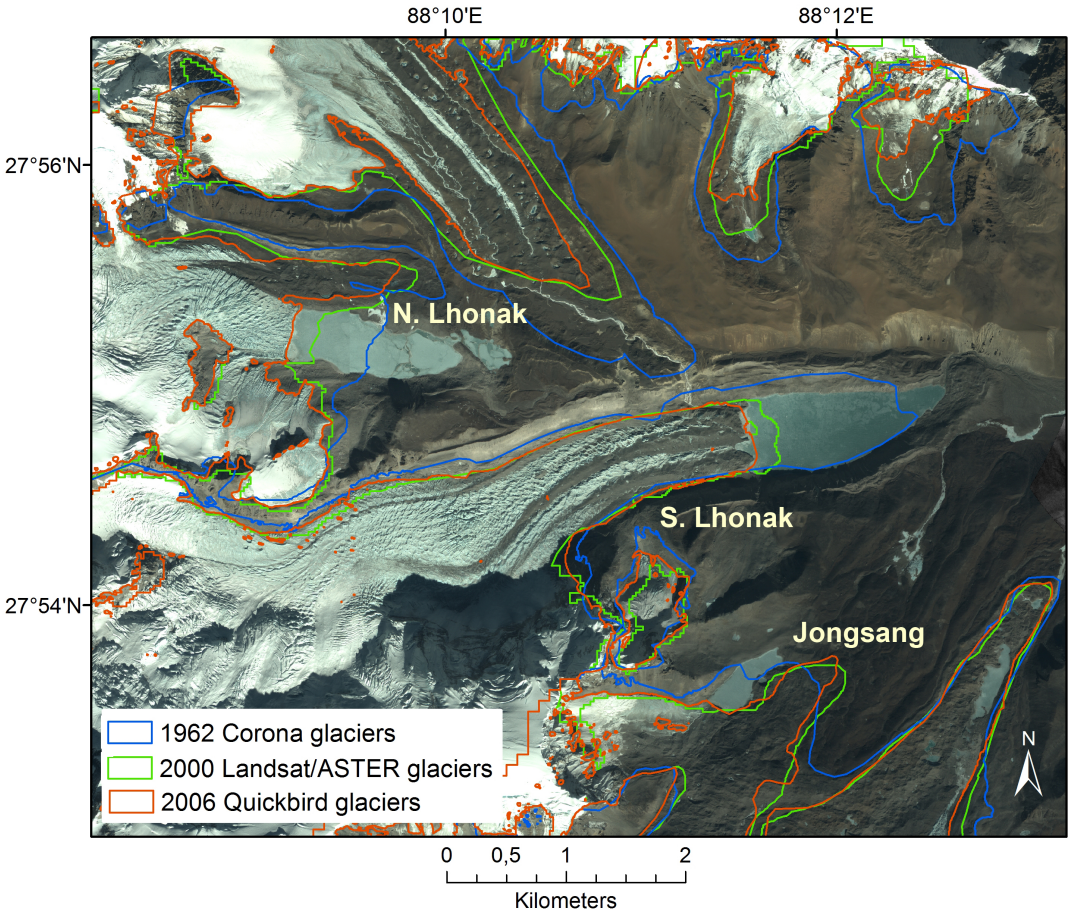
88°10'E
88°12'E
27°56'N
27°54'N
N. Lhonak
S. Lhonak
Jongsang
1962 Corona glaciers
2000 Landsat/ASTER glaciers
2006 Quickbird glaciers
N
0 0,5 1 2
Kilometers

Fig. 11